CHINA CDC WEEKLY

Vol. 7 No. 42 Oct. 17, 2025 Weekly

中国疾病预防控制中心周报



Preplanned Studies

Antibody Levels Against Mumps Virus in Children
After Implementation of the Two-Dose MMR
Vaccine Policy — Fujian Province, China, 2023

1315

Impact of PCV13 Vaccination on Pharyngeal Detection of *Streptococcus pneumoniae* Among Children — Suqian City, Jiangsu Province, China,

February 2023–February 2025

Protective Effect and Immune Mechanism of EPCP009 Booster Immunization after BCG Prime Immunization Against Tuberculosis in Mice — China, 2024

1329

1321

Methods and Applications

Evaluation of Measles Vaccine Immunogenicity and Durability Using A Pseudotyped Virus Neutralization Assay

1337







China CDC Weekly

Editorial Board

Editor-in-Chief Hongbing Shen **Founding Editor** George F. Gao

Deputy Editor-in-Chief Liming Li Gabriel M Leung Zijian Feng

Executive Editor Chihong Zhao **Members of the Editorial Board**

Wen Chen Xi Chen (USA) Zhuo Chen (USA) Rui Chen Ganggiang Ding Xiaoping Dong Pei Gao Mengjie Han Yuantao Hao Na He Yuping He Guoqing Hu Zhibin Hu Weihua Jia Yuegin Huang Na Jia Zhongwei Jia Guangfu Jin Xi Jin Biao Kan Haidong Kan Ni Li Qun Li Ying Li Zhenjun Li Min Liu Qiyong Liu Xiangfeng Lu Jun Lyu Huilai Ma Jiagi Ma Chen Mao Ron Moolenaar (USA) An Pan Xiaoping Miao Daxin Ni Lance Rodewald (USA) William W. Schluter (USA) Yiming Shao Xiaoming Shi Yuelong Shu RJ Simonds (USA) Xuemei Su Chengye Sun Quanfu Sun Xin Sun Feng Tan **Jinling Tang Huaging Wang** Hui Wang Linhong Wang **Tong Wang** Guizhen Wu Jing Wu Xifeng Wu (USA) Yongning Wu Min Xia Ningshao Xia Yankai Xia Lin Xiao Dianke Yu Hongyan Yao Zundong Yin Hongjie Yu Shicheng Yu Ben Zhang Jun Zhang Liubo Zhang Wenhua Zhao Yanlin Zhao Xiaoying Zheng Maigeng Zhou Xiaonong Zhou Guihua Zhuang

Advisory Board

Director of the Advisory Board Jiang Lu

Vice-Director of the Advisory Board Yu Wang Jianjun Liu Jun Yan

Members of the Advisory Board

Chen Fu Gauden Galea (Malta) Dongfeng Gu Qing Gu Yan Guo Ailan Li Jiafa Liu Peilong Liu Yuanli Liu Kai Lu Roberta Ness (USA) **Guang Ning** Minghui Ren Chen Wang Hua Wang Kean Wang Xiaoqi Wang Zijun Wang Fan Wu Xianping Wu

Jingjing Xi Jianguo Xu Gonghuan Yang Tilahun Yilma (USA)

Guang Zeng Xiaopeng Zeng Yonghui Zhang Bin Zou

Editorial Office

Directing Editor Chihong Zhao
Managing Editors Yu Chen

Senior Scientific Editors Daxin Ni Ning Wang Wenwu Yin Jianzhong Zhang Qian Zhu

Scientific Editors

Weihong Chen Tao Jiang Xudong Li Nankun Liu Liwei Shi Liuying Tang Meng Wang Zhihui Wang Qi Yang Qing Yue Lijie Zhang Ying Zhang

Cover Image: credited from the designer Jiaying Wang.

Preplanned Studies

Antibody Levels Against Mumps Virus in Children After Implementation of the Two-Dose MMR Vaccine Policy — Fujian Province, China, 2023

Zhifei Chen^{1,2,&}; Rui Chen^{2,&}; Ruihong Wu^{1,2}; Suhan Zhang¹; Xiuhui Yang^{1,2}; Weiyi Pan¹; Hairong Zhang¹; Mengping Zhang¹; Yong Zhou^{1,2}; Dong Li^{1,2,#}

Summary

What is already known about this topic?

The Measles-Mumps-Rubella (MMR) vaccine plays a crucial role in preventing mumps. Before the implementation of the two-dose MMR vaccine policy, baseline data on mumps virus antibody seroprevalence and geometric mean concentrations (GMCs) among children and adolescents in Fujian Province were available.

What is added by this report?

This report provides a post-policy evaluation following the introduction of Fujian's two-dose MMR policy in June 2020. The 2023 survey shows an overall seroprevalence of 79.53% and a GMC of 265.61 U/mL. Compared with 2018, significant improvements were observed in children under 2 years; however, a concerning decline was noted among adolescents aged 15–17 years. Antibody levels peaked shortly after vaccination, and two doses were found to confer significantly higher immunity than one dose within a 270-day period.

What are the implications for public health practices?

The two-dose MMR policy has been effective in improving early childhood immunity. However, the observed waning immunity in adolescents underscores the urgent need for ongoing serological surveillance, particularly in individuals aged 6–19 years, to inform potential recommendations for booster vaccinations.

ABSTRACT

Introduction: To evaluate population immunity against the mumps virus (MuV) after China's two-dose Measles-Mumps-Rubella (MMR) vaccine policy was introduced in June 2020, we conducted a sero-epidemiological analysis among individuals aged 0–19 years.

Methods: A cross-sectional survey was conducted in Fujian Province from March to June 2023. MuV IgG antibodies were detected using ELISA, and their seroprevalence and geometric mean concentrations (GMCs) were assessed. Population immunity in 2023 was compared with a 2018 survey.

Results: Overall seroprevalence and GMCs in 2023 were 79.53% and 265.61 U/mL, respectively. Both varied significantly by age: levels rose from 8 months, peaked at 2–5 years, then declined to a low point at 15–17 years. In 2023, seroprevalence and GMCs were higher in children aged 0–1 year (47.29% vs. 14.51%; 97.15 U/mL vs. 34.13 U/mL) and lower in those 15–17 years (58.06% vs. 80.73%; 126.00 U/mL vs. 289.98 U/mL) compared with 2018; 2-year-olds showed higher GMCs (554.85 U/mL vs. 353.39 U/mL). Among vaccinated individuals, antibody levels peaked 15–90 days after the latest vaccination; two-dose recipients exhibited significantly higher antibody levels than one-dose recipients within 270 days.

Conclusions: China's two-dose MMR vaccine policy has effectively increased seroprevalence and GMCs in children 8 months-2 years. Continuous monitoring of antibody decline is essential, particularly for those aged 6–19 years with weaker immunity.

Mumps, an acute infectious disease caused by the mumps virus (MuV), is clinically characterized by fever and swelling of the parotid glands and can lead to severe complications, including meningitis, orchitis, sensorineural deafness, myocarditis, pancreatitis, and even death. Although it primarily affects pediatric populations, surveillance data indicate a substantial disease burden among post-pubertal individuals (1). In the absence of specific antiviral therapies, vaccination remains the cornerstone of mumps prevention. Since 2008, a single dose of the trivalent live attenuated

measles-mumps-rubella (MMR) vaccine has been administered at 18 months of age as part of China's national immunization program. However, national surveillance data from 2004 to 2021 show persistent mumps transmission despite vaccination efforts (2). Provincial-level surveillance in Fujian Province from 2014 to 2019 documented approximately 3,200 annual cases, with a bimodal age distribution peaking at 4-6 years and 9-15 years, suggesting suboptimal vaccine effectiveness in school-aged populations (3). Accumulating evidence indicates that a single MMR dose provides only limited long-term protection due to time-dependent waning immunity (4-5). To address this issue, China's National Immunization Program introduced a two-dose MMR policy in 2020, replacing the measles-rubella (MR) vaccine with the MMR vaccine at 8 months, followed by a booster dose at 18 months. From 2020 to 2022, the number of reported mumps cases in Fujian Province showed a continuous decline, with only 1,512 cases reported in 2022 (6). This seroepidemiological study aims to systematically assess population immunity to the mumps virus in 2023 and compare it with baseline data from 2018. These findings will provide actionable insights to guide the optimization of MMR vaccination strategies and support efforts to achieve mumps elimination targets.

In 2023, a cross-sectional serological survey was conducted among individuals aged 0-19 years in Fujian Province, China. Ten counties from ten cities were randomly selected, and two villages communities were randomly chosen from each county. The minimum sample size required for the survey was calculated independently for each city, resulting in a value of N=263. The sample size was determined using the formula: $N=Z_{\alpha}^{2}p(1-p)/d^{2}$, where the parameters were defined as follows: an expected overall mumps seropositivity rate (p) of 0.78 (3), a significance level (α) of 0.05 (Z $_{\alpha}$ =1.96), and an allowable margin of error (d) of 0.05. A systematic sampling method was used to select individuals from each village or community, stratified by age and gender. Individuals with fever, chronic infectious diseases, immunosuppression were excluded. Each participant provided 2-3 mL of venous blood and completed a personal information questionnaire on immunization history. The study was approved by the Fujian Provincial Center for Disease Control and Prevention [Approval No: Fujian Provincial Center for Disease Control and Prevention Ethical Review Approval (2021) No. (016)].

MuV IgG antibodies were detected using

commercial mumps virus IgG ELISA kits (SERION ELISA classic, Institute Virion/Serion GmbH, batch number: EO0014). According to the manufacturer's instructions, samples with concentrations ≥100 U/mL were considered positive, while those with concentrations <100 U/mL were considered negative.

To compare the temporal dynamics of antibody levels following vaccination under two distinct MMR vaccination strategies, we conducted a retrospective cohort study. The study population was drawn from the 2023 and 2018 surveys. The two-dose MMR group included children who received two doses of the MMR vaccine at 8 months and 18 months (2023 survey). The one-dose MMR group consisted of agematched children who had received only a single MMR dose at 18 months (2018 survey). The 2018 survey was a population-based cross-sectional serosurvey conducted in Fujian Province in 2018 and included 4,925 participants aged 0–60 years (3).

Data from the questionnaires were entered into EpiData 3.1 software. Seroprevalence, with corresponding 95% confidence intervals (95% CI), and the GMCs of MuV IgG antibodies were calculated. Differences in seroprevalence and GMCs were assessed using the Chi-square test, Student's t-test, analysis of variance (ANOVA), and Pearson's correlation analysis, as appropriate. Statistical analyses were performed using SPSS Statistics 24.0 and GraphPad Prism 8.0.1, with two-sided P-values <0.05 considered statistically significant.

A total of 2,711 subjects aged 0-19 years were recruited. The overall seroprevalence was 79.53% (95% CI: 78.01%-81.05%), and the GMC was 265.61 U/mL (95% CI: 253.79-278.55 U/mL). Both seroprevalence and GMCs differed significantly across and vaccination statuses. groups Among individuals aged 0-19 years, seroprevalence ranged from 22.06% to 96.10%, and GMCs ranged from 53.88 U/mL to 554.85 U/mL (Table 1). The lowest seroprevalence was observed in the 0-7-month age group ($0 \le \text{to } < 8 \text{ months}$), peaking among those aged 2-5 years and then gradually declining in the 15-17year age group (15≤ to <18 years). Seroprevalence among individuals aged 2-17 years showed a significant downward trend (χ^2 =268.30, P<0.001). GMCs were 53.88 U/mL at 0-7 months, rose sharply to 263.09 U/mL between 8 months and 1 year, and peaked at 554.85 U/mL at age 2. Thereafter, GMCs gradually declined to a low of 126.00 U/mL over the next 15 years. Notably, GMCs among individuals aged 2-17 years demonstrated a negative correlation with

TABLE 1. Seroprevalence and GMCs of MuV IgG by gender, age, and vaccination status among individuals among aged 0–19 years in Fujian Province in 2023.

Characteristic	Sample No.	Seroprevalence % (95% CI)	χ^2 , P	GMCs (95% CI) (U/mL)	t/F, P
Gender					
Male	1,475	79.53 (77.46, 81.59)	0.00,	261.83 (247.03, 278.99)	0.664,
Female	1,236	79.53 (77.28, 81.78)	1.000	270.19 (252.17, 289.93)	0.507
Age					
0≤ to <8 months	68	22.06 (11.95, 32.17)		53.88 (41.54, 70.26)	
8≤ to <24 months	479	76.00 (72.15, 79.83)		263.09 (228.11, 302.75)	
2≤ to <3 years	270	95.19 (92.62, 97.76)		554.85 (495.81, 616.27)	
3≤ to <4 years	263	93.92 (91.01, 96.82)		419.99 (378.88, 464.68)	98.54, <0.001
4≤ to <5 years	287	94.08 (91.33, 96.82)		442.89 (399.13, 489.03)	
5≤ to <6 years	282	96.10 (93.83, 98.37)	480.99, <0.001	425.59 (385.74, 464.15)	
6≤ to <12 years	267	85.02 (80.71, 89.33)	10.001	289.94 (258.78, 324.09)	
12≤ to <15 years	241	70.12 (64.30, 75.94)		150.10 (133.47, 169.88)	
15≤ to <18 years	279	58.06 (52.24, 63.89)		126.00 (110.80, 144.01)	
18≤ to <20 years	275	63.27 (57.54, 69.01)		146.39 (128.10, 166.20)	
Total	2,711	79.53 (78.01, 81.05)		265.61 (253.79, 278.55)	
Vaccination status					
0 dose	208	31.25 (24.9, 37.60)		58.84 (49.01, 70.51)	
1 dose	1,283	83.63 (81.60, 85.66)	516.26,	270.66 (256.39, 286.74)	305.60,
≥2 dose	753	96.15 (94.77, 97.53)	<0.001	567.22 (528.34, 600.82)	<0.001
Unknown	237	59.92 (53.63, 66.20)		136.61 (118.03, 159.75)	
Total	2,481	80.77 (79.22, 82.33)		279.27 (265.87, 292.17)	

Abbreviation: GMC=geometric mean concentration; CI=confidence intervals.

Note: Seroprevalence among different groups was compared using the chi-square test. For GMCs, comparisons between two groups were analyzed using the t-test, and comparisons among three or more groups were assessed using analysis of variance (ANOVA).

age by Pearson correlation analysis (r=-0.47, P<0.001).

A total of 2,481 subjects completed questionnaires regarding their mumps-containing vaccine history. Based on vaccination status, the distribution of individuals receiving 0 doses, 1 dose, \geq 2 doses, and unknown status was 8.38%, 51.71%, 30.35%, and 9.55%, respectively. Seroprevalence and GMCs in vaccinated children were significantly higher than in unvaccinated children. Furthermore, children who received \geq 2 doses of the vaccine exhibited higher seroprevalence and GMCs than those who received only 1 dose.

Due to differing age distributions between the two studies, we calculated standardized seroprevalence estimates of MuV IgG for 2023 and 2018. The seroprevalence and GMCs in the 2023 study population (79.53%, 265.61 U/mL) were significantly higher than those in the 2018 population (74.65%, 229.06 U/mL) (χ^2 =20.09, P<0.001; t=4.47, P<0.001). In the 0–1-year age group, seroprevalence

and GMCs in 2018 (14.51%, 34.13 U/mL) were significantly lower than those in 2023 (47.29%, U/mL) ($\chi^2 = 74.90$, P < 0.001; t = 9.314, P<0.001). Both surveys showed high seroprevalence in the 2-5-year age group, followed by a gradual decline beginning at age 6. A notable decrease was observed in adolescents aged 15-17, with seroprevalence and GMCs in 2023 significantly lower than those in the corresponding age group in 2018 (80.73%, 289.98 U/mL) (χ^2 =37.053, P<0.001; t=8.978, P<0.001). GMCs for 2-year-olds in 2023 were also significantly higher than those for the same age group in 2018 (353.39 U/mL) (t=5.916, P<0.001). Both studies demonstrated a declining trend in GMCs over time, with a notable widening of the disparity between the two cohorts after age 12, as markedly lower GMCs were recorded in 2023 compared with 2018 (Figure 1).

In the 2023 survey, we identified 329 participants (male: 57.14%; female: 42.86%) aged 1.5–4 years (median: 2.45 years) who had received two doses of the

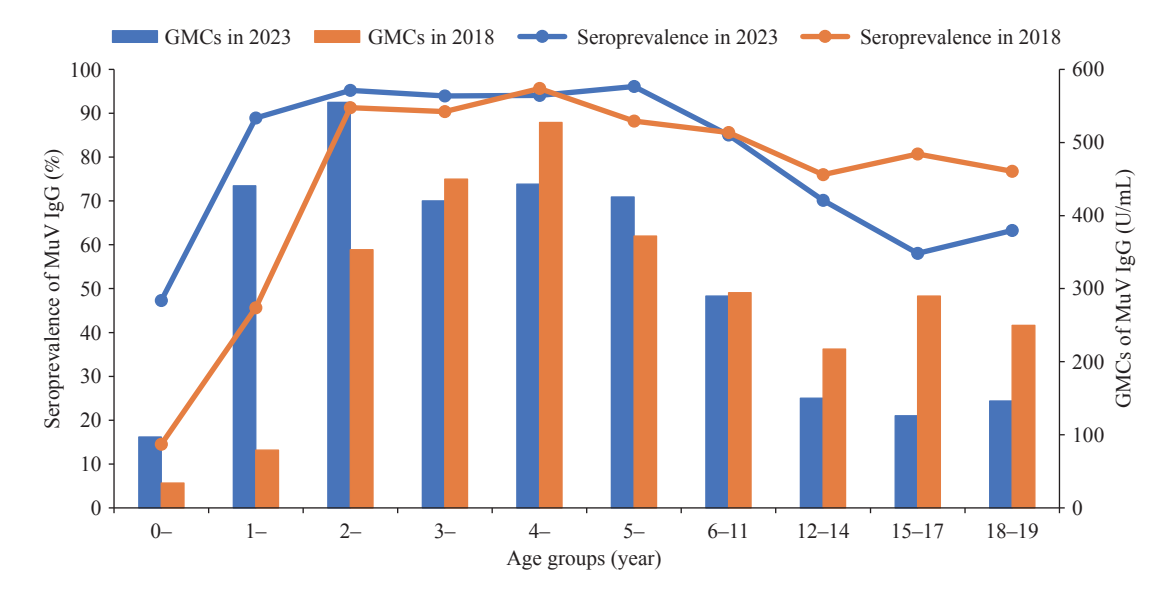


FIGURE 1. Seroprevalence and GMCs of MuV IgG in 2023 and 2018.

Note: The figure shows mumps antibody levels across various age groups in 2023 and 2018. Blue bars represent the GMCs of mumps antibodies in 2023, while orange bars represent the corresponding GMCs in 2018. The blue line indicates the seropositivity rate of mumps antibodies in 2023, and the orange line shows the seropositivity rate in 2018.

Abbreviation: GMC=geometric mean concentration.

MMR vaccine at 8 months and 18 months, respectively. The interval since the second dose ranged from 0 to 1,079 days (median: 303 days). Additionally, we identified 557 participants (male: 56.91%; female: 43.09%) aged 1.5–4 years (median: 2.70 years) from the 2018 survey who had received a single MMR dose at 18 months. The interval since vaccination in this group ranged from 0 to 885 days (median: 385 days). Based on the time since vaccination, participants were categorized into eight intervals: 0–14, 15–90, 91–180, 181–270, 271–360, 361–450, 451–540, 541–630, 631–720, and 721–1,079 days post-vaccination.

Among participants who received two MMR doses, GMCs were 204.12 U/mL within 0-14 days postvaccination, peaked at 1468.12 U/mL between 15 and 90 days, and then declined to 516.39 U/mL at 271-360 days. Thereafter, GMCs remained relatively fluctuating between 502.69 U/mL and 693.80 U/mL. A similar pattern was observed in participants who received one MMR dose, with GMCs increasing from 32.74 U/mL at 0-14 days to 434.89 U/mL at 15-90 days, followed by a steady plateau. Antibody levels in two-dose recipients within 270 days of the last vaccination were significantly higher than those in one-dose recipients (P<0.001). However, this difference gradually diminished, with levels approaching similarity by 271-360 days postvaccination (Figure 2).

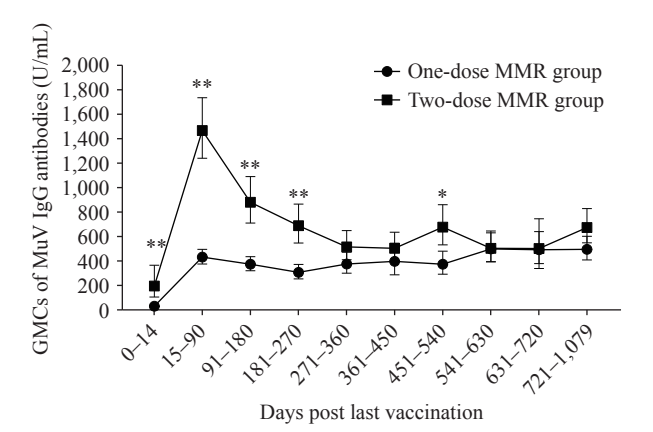


FIGURE 2. Dynamic changes in MuV IgG antibody levels following vaccination with different doses of the MMR vaccine.

Note: The figure presents the GMCs of MuV IgG antibodies in populations that received two different MMR vaccination regimens, measured at multiple time points after vaccination. The dotted line represents the temporal changes in antibody levels among individuals in the one-dose MMR group, while the square-marked line shows the corresponding dynamics in the two-dose MMR group.

Statistical significance between the two groups is indicated by asterisks: **P*<0.01 and ***P*<0.001.

Abbreviation: GMC=geometric mean concentration; MMR=measles-mumps-rubella.

DISCUSSION

This study examined mumps virus antibody levels in children aged 0–19 years in Fujian Province, three

years after the implementation of the two-dose MMR vaccine policy in 2020. Compared with data from 2018, overall antibody levels showed a slight increase in 2023, with the most substantial improvement observed in children aged 8 months-2 years. In this age group, both seroprevalence (rising from 76.00% to 95.19%) and GMCs (increasing from 263.09 to 554.85 U/mL) improved markedly. Children aged 3-5 maintained high antibody levels, seroprevalence ranging from 93.92% to 96.10% and GMCs between 419.99 and 442.89 U/mL. However, antibody levels began to decline gradually from 6 years of age onward. In 2-year-olds, antibody levels induced by two MMR doses were significantly higher than those generated by a single dose. Nevertheless, within 360 days after the second dose, antibody levels gradually decreased to levels comparable to those in children who had received only one dose (MMR1).

studies have reported immunological boost in MuV antibodies following a second (MMR2) or third (MMR3) dose of the MMR vaccine is temporary, with antibody levels returning to pre-boost levels within approximately one year (7–8). Our study confirms this finding: MuV antibody levels initially rose in response to MMR2 but declined to near MMR1 levels within one year. The transient nature of this boost may be attributed to the low frequency of mumps-specific memory B cells generated after MMR vaccination, which fails to establish strong long-term B-cell memory (9). Despite the post-MMR2 decline in antibody levels, children aged 3-5 years still maintained sufficient levels to support high herd immunity against mumps.

It is noteworthy that there has been a continuous decline in antibody levels among individuals aged 6-19 years who received only one dose of the MMR vaccine, placing them in a high-risk window for mumps infection. Their seroprevalence ranged from 58.06% to 85.02%, significantly lower than the estimated herd immunity threshold of 88%-92% (10). Children aged 15-17 years, the first cohort to receive the MMR vaccine under the Expanded Program Immunization (EPI), have become a particularly vulnerable population in 2023, as reflected by a relatively low seroprevalence of 58.06% and antibody titers of 126 U/mL. In contrast, their seroprevalence and GMCs in 2018 were 80.73% and 289.98 U/mL, respectively, indicating a marked decline. Furthermore, high contact rates and population density in primary and senior high schools may facilitate mumps transmission, potentially overcoming vaccine-induced

protection among students (11). Notably, most outbreaks in primary and junior high schools have occurred in populations with high vaccination coverage (12–13). Between 2017 and 2021, 72.92% of mumps cases in individuals under 18 years old were breakthrough infections, with this proportion rising to 90.78% in 2021 in Huzhou City, China (14). Numerous studies have confirmed that students who received their last dose of a mumps-containing vaccine (MuCV) more than 10 years before an outbreak face an increased risk of contracting mumps (12,15).

The study has certain limitations. First, it was conducted only three years after the implementation of the two-dose MMR vaccination program, which limits our ability to capture long-term serological dynamics in vaccinated populations. Second, although a cohort study would be optimal for tracking antibody kinetics across multiple time points post-vaccination, this research used a cross-sectional design, which is primarily descriptive and serves as an early warning signal. Additionally, cross-sectional studies cannot distinguish antibody increases caused by natural infection after vaccination, which may lead to an overestimation of vaccine-induced protection.

In conclusion, the implementation of the two-dose MMR vaccination policy has resulted in high seroprevalence and GMCs among children aged 8 months to 2 years. However, continuous monitoring of antibody waning is essential. Enhanced surveillance of mumps in children and adolescents aged 6–19 years is also critical due to their relatively low antibody levels.

Conflicts of interest: No conflicts of interest.

Acknowledgements: All the unnamed participants in this study, particularly the CDC staff at all levels who were involved in the serosurvey.

Funding: Supported by the Talent Training Project of Fujian Provincial Health Commission (2021GGB011).

doi: 10.46234/ccdcw2025.223

Copyright © 2025 by Chinese Center for Disease Control and Prevention. All content is distributed under a Creative Commons Attribution Non Commercial License 4.0 (CC BY-NC).

Submitted: July 22, 2025 Accepted: September 25, 2025 Issued: October 17, 2025

^{*}Corresponding author: Dong Li, lidong@fjcdc.com.cn.

¹ Fujian Provincial Key Laboratory of Zoonosis Research, Fujian Provincial Center for Disease Control and Prevention, Fuzhou City, Fujian Province, China; ² School of Public Health, Fujian Medical University, Fuzhou City, Fujian Province, China.

[&]amp; Joint first authors.

REFERENCES

- Ohfuji S, Takagi A, Nakano T, Kumihashi H, Kano M, Tanaka T. Mumps-related disease burden in Japan: analysis of JMDC health insurance reimbursement data for 2005-2017. J Epidemiol 2021;31(8): 464 – 70. https://doi.org/10.2188/jea.JE20200048.
- Li P, Wang FZ, Yang H, Huang AD, Ma C, Yin ZD. Epidemiological characteristics and spatial-temporal clustering of mumps in China, 2004-2021. Chin J Vaccines Immun 2023;29(1):19 – 24. https://doi. org/10.19914/i.CJVI.2023004.
- Li D, Zhang HR, You N, Chen ZF, Yang XH, Zhang HS, et al. Mumps serological surveillance following 10 years of a one-dose mumps-containing-vaccine policy in Fujian Province, China. Hum Vaccin Immunother 2022;18(6):2096375. https://doi.org/10.1080/ 21645515.2022.2096375.
- Sun X, Tang FY, Hu Y, Deng XY, Wang ZG, Zhou MH, et al. High risk of mumps infection in children who received one dose of mumpscontaining vaccine: waning immunity to mumps in children aged 2-5 years from kindergartens in Jiangsu Province, China. Hum Vaccin Immunother 2020;16(7):1738 – 42. https://doi.org/10.1080/ 21645515.2019.1708162.
- Yin ZY, Wen TC, Fang QJ, Zheng CJ, Gong XY, Li JJ, et al. Assessment of mumps-containing vaccine effectiveness by dose during 2006 to 2020 in Quzhou, China. Hum Vaccin Immunother 2022;18 (5):2086774. https://doi.org/10.1080/21645515.2022.2086774.
- Wu RH, Chen ZF, Yang XH, Chen YH, Chen DH, Zhang HR, et al. Investigating the characteristics of mumps outbreaks in Fujian Province, China. Vaccine 2024;42(26):126415. https://doi.org/10.1016/j.vaccine. 2024 126415
- Fiebelkorn AP, Coleman LA, Belongia EA, Freeman SK, York D, Bi DL, et al. Mumps antibody response in young adults after a third dose of measles-mumps-rubella vaccine. Open Forum Infect Dis 2014;1(3): ofu094. https://doi.org/10.1093/ofid/ofu094.
- 8. Sarawanangkoor N, Wanlapakorn N, Srimuan D, Thatsanathorn T,

- Thongmee T, Poovorawan Y. Persistence of antibodies against measles, mumps, and rubella after the two-dose MMR vaccination: a 7-year follow-up study. Vaccines 2024;12(7):744. https://doi.org/10.3390/vaccines12070744.
- Rasheed MAU, Hickman CJ, McGrew M, Sowers SB, Mercader S, Hopkins A, et al. Decreased humoral immunity to mumps in young adults immunized with MMR vaccine in childhood. Proc Natl Acad Sci USA 2019;116(38):19071 – 6. https://doi.org/10.1073/pnas. 1905570116.
- Anderson RM, May RM. Vaccination and herd immunity to infectious diseases. Nature 1985;318(6044):323 – 9. https://doi.org/10.1038/ 318323a0.
- 11. Barskey AE, Schulte C, Rosen JB, Handschur EF, Rausch-Phung E, Doll MK, et al. Mumps outbreak in Orthodox Jewish communities in the United States. N Engl J Med 2012;367(18):1704 13. https://doi.org/10.1056/NEJMoa1202865.
- Qin W, Wang Y, Yang T, Xu XK, Meng XM, Zhao CJ, et al. Outbreak of mumps in a student population with high vaccination coverage in China: time for two-dose vaccination. Hum Vaccin Immunother 2019;15(9):2106 – 11. https://doi.org/10.1080/21645515.2019. 1581526
- Wang DN, Nie TY, Pan F, Wang Y, Wang J, Qin W. Loss of protective immunity of two-dose mumps-containing vaccine over time: concerns with the new strategy of the mumps immunization program in China. Hum Vaccin Immunother 2021;17(7):2072 – 7. https://doi. org/10.1080/21645515.2020.1861877.
- Zhang C, Shen JY, Luo XF, Han LP. Epidemiological characteristics of breakthrough cases of breakthrough mumps cases among children under eighteen years old between 2017 and 2021 in Huzhou City. China Modern Doctor 2023;61(26):70 – 3,78. https://doi.org/10.3969/j.issn. 1673-9701 2023 26 014
- Cardemil CV, Dahl RM, James L, Wannemuehler K, Gary HE, Shah M, et al. Effectiveness of a third dose of MMR vaccine for mumps outbreak control. N Engl J Med 2017;377(10):947 – 56. https://doi. org/10.1056/NEJMoa1703309.

Preplanned Studies

Impact of PCV13 Vaccination on Pharyngeal Detection of Streptococcus pneumoniae Among Children — Suqian City, Jiangsu Province, China, February 2023–February 2025

Lisha Ma^{1,&}; Mingwei Wei^{2,3,&}; Tao Wu³; Ran Tao³; Jinbo Gou⁴; Yue Liu¹; Manrong Zhang¹; Mengjuan Yuan²; Lunbiao Cui³,[#]; Jingxin Li¹,^{3,#}

Summary

What is already known on this topic?

Pneumococcal conjugate vaccines (PCVs), including the 13-valent PCV (PCV13), effectively reduce the nasopharyngeal carriage of vaccine-type *Streptococcus pneumoniae* (*S. pneumoniae*) and prevent invasive pneumococcal disease in children. However, an increasing prevalence of non-vaccine serotypes and serotype replacement has been documented globally, with notable variations in the predominant replacement serotypes across different geographic settings.

What is added by this report?

This study demonstrated that PCV13 vaccination significantly reduced the pharyngeal detection of *S. pneumoniae* among children with acute respiratory infections, with three to four doses decreasing the detection rate by 30.2%. This reduction encompassed both vaccine and non-vaccine serotypes. Additionally, non-PCV13 serotypes, particularly 10A and 15A/15F, were predominant in positive samples, underscoring the current dominance of non-vaccine serotypes in the study population.

What are the implications for public health practice?

The PCV13 program successfully reduced pneumococcal detection rates, particularly among children who complete the 3–4 dose series. Continued surveillance of circulating *S. pneumoniae* serotypes is essential to monitor serotype replacement patterns and develop future vaccination strategies.

ABSTRACT

Introduction: The 13-valent pneumococcal conjugate vaccine (PCV13) has reduced vaccine-type carriage rates, though regarding serotype replacement remain.

Methods: This study conducted a 2-year prospective cohort study (February 2023–February 2025) in Suqian, Jiangsu Province, enrolling 2-month-old infants and monitoring for acute respiratory infections (ARIs). Pharyngeal swabs collected during ARIs were analyzed using targeted next-generation sequencing (tNGS) to identify respiratory pathogens, and *Streptococcus pneumoniae* (S. pneumoniae)-positive samples were serotyped using multiplex PCR. Risk ratios (RRs) for S. pneumoniae detection were estimated using Poisson regression, with sensitivity analysis performed using inverse probability of treatment weighting (IPTW).

Results: Among 579 children, 1,527 swabs were collected, yielding an overall *S. pneumoniae* detection incidence of 35.2%. Vaccinated children receiving 3–4 PCV13 doses demonstrated significantly lower detection rates than unvaccinated children [23.1% *vs.* 40.2%; adjusted *RR*=0.70; 95% confidence interval (*CI*): 0.50, 0.98; *P*=0.036]. IPTW analysis confirmed these findings. Non-vaccine serotypes predominated, particularly the 10A and 15A/15F strains.

Conclusion: PCV13 vaccination was associated with reduced *S. pneumoniae* detection among children with ARIs, despite dominance of non-vaccine serotypes. Our findings emphasize the importance of ongoing surveillance for *S. pneumoniae* and highlight the need to expand the serotype coverage of pneumococcal vaccines.

Streptococcus pneumoniae (S. pneumoniae) represents a major bacterial pathogen responsible for significant infections and mortality among children under five years of age. Nasopharyngeal colonization serves not only as the primary reservoir for horizontal transmission within communities but also as an essential prerequisite for invasive disease development

(1). Young children serve as the principal reservoir, with point prevalence estimates of nasopharyngeal colonization ranging from 27% to 85% (2). The introduction of pneumococcal conjugate vaccines (PCVs) has substantially reduced the incidence of vaccine-type carriage and pneumococcal disease among young children. However, the selective pressure exerted by vaccination has fundamentally altered the microbial landscape, resulting in an increased prevalence of nonvaccine serotypes, with a growing proportion of infections now attributed to replacement serotypes, such as 8, 10A, 12F, 15A, and 24F (3). In recent years, global interest has intensified regarding the protective effects of PCVs and the associated changes in pneumococcal serotype distribution across diverse populations. Therefore, based on a prospective acute respiratory infection (ARI) surveillance cohort in eastern China, the present study aimed to evaluate the impact of PCV13 vaccination on the risk of S. pneumoniae detection and characterize the current distribution of predominant pneumococcal serotypes among young children.

This study was based on a prospective cohort of healthy infants established in February 2023 in Sugian, Jiangsu Province, Eastern China, as previously reported (4). Briefly, infants aged 2 months at recruitment were enrolled and actively monitored for ARI episodes over 24 months. Demographic data and baseline pharyngeal swabs were collected at enrollment. During the surveillance, the researchers contacted caregivers biweekly via telephone to monitor their health status. When a child exhibited ARI symptoms such as cough, nasal congestion, tachypnea, or throat redness and swelling, researchers conducted home visits within 48 hours to collect pharyngeal swabs. Trained healthcare personnel collected pharyngeal swabs. With the child's head tilted slightly backward, a disposable flocked swab was inserted into the posterior pharyngeal wall and tonsillar areas, rotated 3-5 times, and immediately placed in a tube containing the viral transport medium. All specimens were transported on dry ice and stored at -80 °C prior to laboratory testing.

Pharyngeal swab specimens were analyzed using the (KS608-Respiratory Pathogen Detection Kit 100HXD96, KingCreate, Guangzhou, China) for targeted next-generation sequencing (tNGS), which can identify 107 respiratory pathogens, including S. pneumoniae, Mycoplasma pneumoniae, and influenza A and B viruses. Detailed tNGS procedures are provided the Supplementary Material (available https://weekly.chinacdc.cn/). Serotyping was

performed using multiplex PCR for specimens that tested positive for *S. pneumoniae*. DNA extraction and analysis of the amplified products from earlier surveys have been described previously (4). PCV13 vaccination status during the follow-up period was obtained from the National Immunization Information System.

All statistical analyses were conducted using the R Software (version 4.4.1; The R Foundation for Statistical Computing, Vienna, Austria). Descriptive statistics, including medians, interquartile ranges (IQRs), and percentages, were calculated to summarize the baseline characteristics of the study population. Categorical variables were compared using the Chisquare test, and continuous variables were compared using the Mann-Whitney U test. We compared the overall incidence of S. pneumoniae detection in PCV13-vaccinated and unvaccinated children. Risk ratios (RRs) were estimated using Poisson regression with robust standard errors by PCV13 doses, and adjusted RRs were obtained after controlling for sex, disease history, mode of delivery, maternal age at delivery, maternal education level, maternal monthly income, number of household members, presence of children under 18 years of age in the household, household income, and monthly baseline pneumoniae carriage. We employed inverse probability of treatment weighting (IPTW) using propensity scores to reconstruct comparable cohorts of PCV13vaccinated and unvaccinated individuals for sensitivity analysis to examine the impact of PCV13 on the detection of S. pneumoniae. The reduction in pneumococcal occurrence attributable to vaccination was calculated as (1-adjusted RR)×100%. For samples with failed serotyping, multiple imputations were applied using chained equations. Missing serotype values were imputed using classification and regression tree methods to generate 20 imputed datasets. The results from all the imputed datasets were subsequently combined using Rubin's rules. A two-sided P value of < 0.05 was considered statistically significant.

Of the 796 children enrolled in the longitudinal ARI surveillance cohort study, 579 (72.7%) provided at least one valid pharyngeal swab sample during an ARI episode and were included in the present analysis. The baseline demographic characteristics of the 579 participants did not differ significantly from those of the overall cohort (Supplementary Table S1, available at https://weekly.chinacdc.cn/). Among the included children, 310 (53.5%) were boys, 21 (3.6%) carried *S. pneumoniae* at enrollment, and 54 (9.3%) received one dose of PCV13 before enrollment (Table 1).

TABLE 1. Baseline demographic characteristics of 579 participants analyzed in this study.

Characteristics	Participants included in the analysis
Infant sex, n (%)	
Female	269 (46.5)
Male	310 (53.5)
Infant age, median (IQR), days	71.0 (66.0, 78.0)
Infant height, median (IQR), cm	60.0 (59.0, 62.0)
Infant weight, median (IQR), kg	6.3 (5.8, 6.8)
Infant birth length, median (IQR), cm	50.0 (50.0, 50.0)
Infant birth weight, median (IQR), kg	3.4 (3.2, 3.7)
nfant disease history*, n (%)	
Yes	18 (3.1)
No	561 (96.9)
Maternal mode of delivery, n (%)	
Full-term vaginal delivery	291 (50.3)
Cesarean delivery	288 (49.7)
Maternal feeding pattern, n (%)	
Breastfeeding	523 (90.3)
Not breastfeeding after birth	47 (8.1)
Mixed feeding	9 (1.6)
Maternal age, n (%), years	
<35	503 (86.9)
≥35	76 (13.1)
Maternal education, n (%)	
Middle school or below	162 (28.0)
High school or vocational school	100 (17.3)
Junior college	152 (26.3)
Bachelor's degree or above	165 (28.5)
Maternal monthly income, n (%), CNY	
<1,000	245 (42.3)
1,000-6,999	270 (46.6)
≥7,000	64 (11.1)
No. of household members, n (%)	
≤4	421 (72.7)
>4	158 (27.3)
Nith household members <18 years of age, n (%)	
Yes	329 (56.8)
No	250 (43.2)
Monthly household income, n (%), CNY	
<10,000	175 (30.2)
≥10,000	404 (69.8)
Baseline S. pneumoniae carriage	
Yes	21 (3.6)
No	553 (95.5)
Missing	5 (0.9)
Received first dose of PCV13 before enrollment, n (%)	• •
Yes	54 (9.3)
No	525 (90.7)

Abbreviation: PCV13=13-valent pneumococcal conjugate vaccine; CNY=Chinese Yuan; COVID-19=coronavirus disease 2019.

^{*} Infant disease history includes pneumonia, jaundice, COVID-19, and lactose intolerance.

During the study period, 2,996 ARI episodes were recorded, yielding an incidence rate of 196.6 episodes per 100 person-years (95% CI: 189.5, 203.6). A total of 1,527 pharyngeal swab samples were collected from 579 participants. Among them, 204 tested positive for S. pneumoniae at least once, with an overall detection rate of 35.2% (95% CI: 31.3%, 39.1%). Overall, 181 (31.3%) children received 1–4 doses of PCV13, whereas 398 (68.7%) remained unvaccinated. Notably, PCV13 vaccination was not associated with a reduction in the overall ARI incidence (Table 2).

For each of the 204 children with S. pneumoniae, one positive sample was randomly selected for serotyping analysis. Of these, 137 (67.2%) were successfully serotyped. Among the 137 successfully serotyped samples, 105 (76.6%) contained a single serotype, 26 (19.0%) contained two serotypes, and 6 (4.4%) contained three serotypes. The most frequently detected non-vaccine serotypes were 10A (30.3%) and 15A/15F (22.3%), with 23F (3.4%) being the most common (Figure 1). For samples for which serotyping failed, we additionally applied multiple imputations that showed a consistent serotype distribution. The detection rates of most non-vaccine serotypes were higher in unvaccinated children than in vaccinated children. Statistically significant differences were observed for serotypes 10A (P=0.041) and 15A/15F (P=0.003) based on the Pearson's Chi-square test, whereas no significant differences were detected for the other serotypes (Figure 2).

Among children in the overall pneumococcal group, those who received 1–2 doses of PCV13 demonstrated an incidence of *S. pneumoniae* detection of 28.9% (95% *CI*: 15.4%, 45.9%), compared to 40.2% (95% *CI*: 35.3%, 45.2%) in unvaccinated children, with an adjusted RR of 0.80 (95% *CI*: 0.49, 1.32; P=0.392) (Table 3). In contrast, children who received 3–4 doses exhibited a 30.2% reduction in *S. pneumoniae* detection (adjusted RR=0.70; 95% *CI*: 0.50, 0.98; P=0.036). A significant 39.0% reduction in nonvaccine-type *S. pneumoniae* detection was also observed in this group (adjusted RR=0.61; 95% *CI*: 0.38, 0.97; P=0.037) (Table 3). Owing to the limited sample size,

no significant effect of PCV13 was observed on vaccine-type *S. pneumoniae* detection, although point estimates suggested some differences. Sensitivity analyses using IPTW yielded consistent results, demonstrating a 61.9% reduction in non-vaccine-type *S. pneumoniae* detection (*RR*=0.38; 95% *CI*: 0.23, 0.64; *P*<0.001) (Table 3).

DISCUSSION

This study evaluated the impact of PCV13 vaccination on the detection of S. pneumoniae among children with ARI through a comprehensive 24-month active surveillance program. During the follow-up period, the overall incidence of S. pneumoniae detection was 35.2%. Children who received 3-4 doses of PCV13 demonstrated a significantly reduced risk of S. pneumoniae detection compared with their unvaccinated counterparts, with particularly pronounced reductions observed for non-vaccine serotypes 10A and 15A/15F.

The detection rate of *S. pneumoniae* observed in our cohort was 35.2%, exceeding that reported in previous studies of healthy children under 5 years of age (30.4%) (5) and the pooled prevalence estimate from a recent meta-analysis of Chinese children (21.4%) (6). This elevated detection rate can be attributed to our prospective cohort design, which enabled the comprehensive identification of ARI episodes and the implementation of tNGS, a highly sensitive molecular technique that achieves superior detection rates compared with traditional culture-based methods.

Our findings demonstrated that PCV13 vaccination significantly reduced the risk of pneumococcal detection during childhood, particularly among children who completed the 3–4 dose immunization series, reflecting the direct protective effect of the vaccine on vaccinated individuals. However, no significant effect was observed on the overall incidence of ARI. Unlike previous studies that primarily focused on vaccine serotypes, our results suggest that PCV13 vaccination may also be associated with a reduced detection of non-vaccine serotypes. Following the

TABLE 2. Incidence of acute respiratory infection episodes per 100 person-years by PCV13 vaccination status.

PCV13 vaccination status	Person years	No. of events	Rate (95% CI)	Incidence rate ratio (95% CI)	P
Unvaccinated	819	1,676	204.6 (194.8, 214.4)	Reference	-
1-2 doses	78	150	191.9 (161.2, 222.6)	0.94 (0.79, 1.10)	0.448
3-4 doses	294	591	201.0 (184.8, 217.2)	0.98 (0.89, 1.08)	0.695

Note: The incidence rate ratio and 95% *CI* were estimated using Poisson regression models with log (person-years) as the offset. Abbreviation: PCV13=13-valent pneumococcal conjugate vaccine; *CI*=confidence interval.

China CDC Weekly

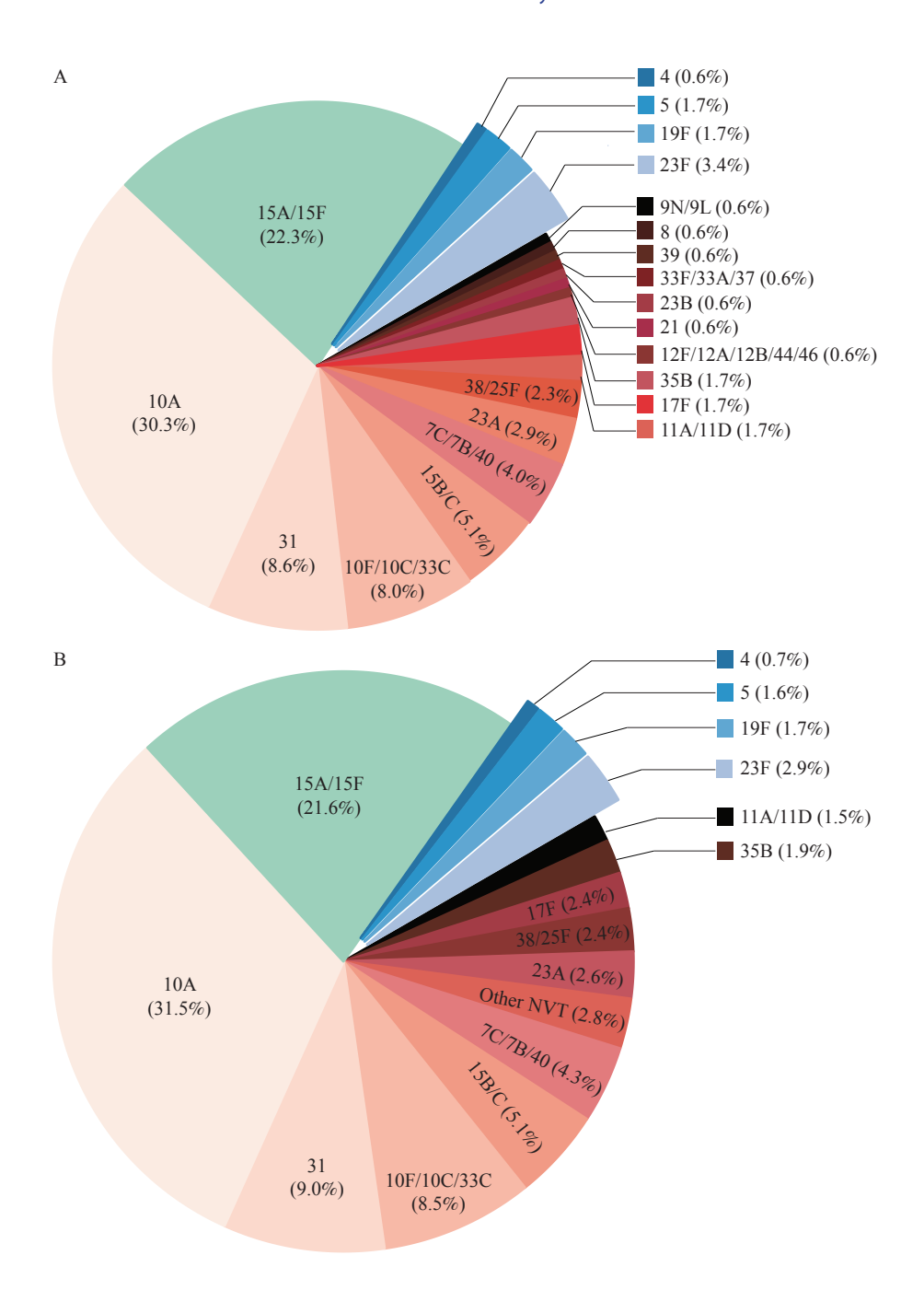


FIGURE 1. Distribution of pneumococcal serotypes during ARI episodes among children. (A) Serotype distribution of Streptococcus pneumoniae detected during ARI episodes; (B) Serotype distribution of Streptococcus pneumoniae after multiple imputation.

Note: In panels A and B, the vaccine serotypes are highlighted in blue. Other NVT included 12F/12A/12B/44/46, 21, 23B, 33F/33A/37, 39, 8, and 9N/9L.

Abbreviation: NVT=non-vaccine serotypes; ARI=acute respiratory infection.

introduction of PCVs, vaccine-type serotypes are markedly suppressed, whereas non-vaccine serotypes may not colonize efficiently, and therefore may not fully occupy the niche vacated by vaccine types, leaving ecological space for competing colonizers (7). In a randomized controlled trial on PCV7, a negative association in co-colonization between *S. pneumoniae*

(both vaccine-type and non-vaccine serotypes) and *Staphylococcus aureus* was observed (8).

Our results also revealed that non-vaccine serotypes of *S. pneumoniae* were predominant over vaccine serotypes, with serotypes 10A and 15A/15F being the most prevalent, whereas vaccine serotypes accounted for only 7.4%. These findings are consistent with

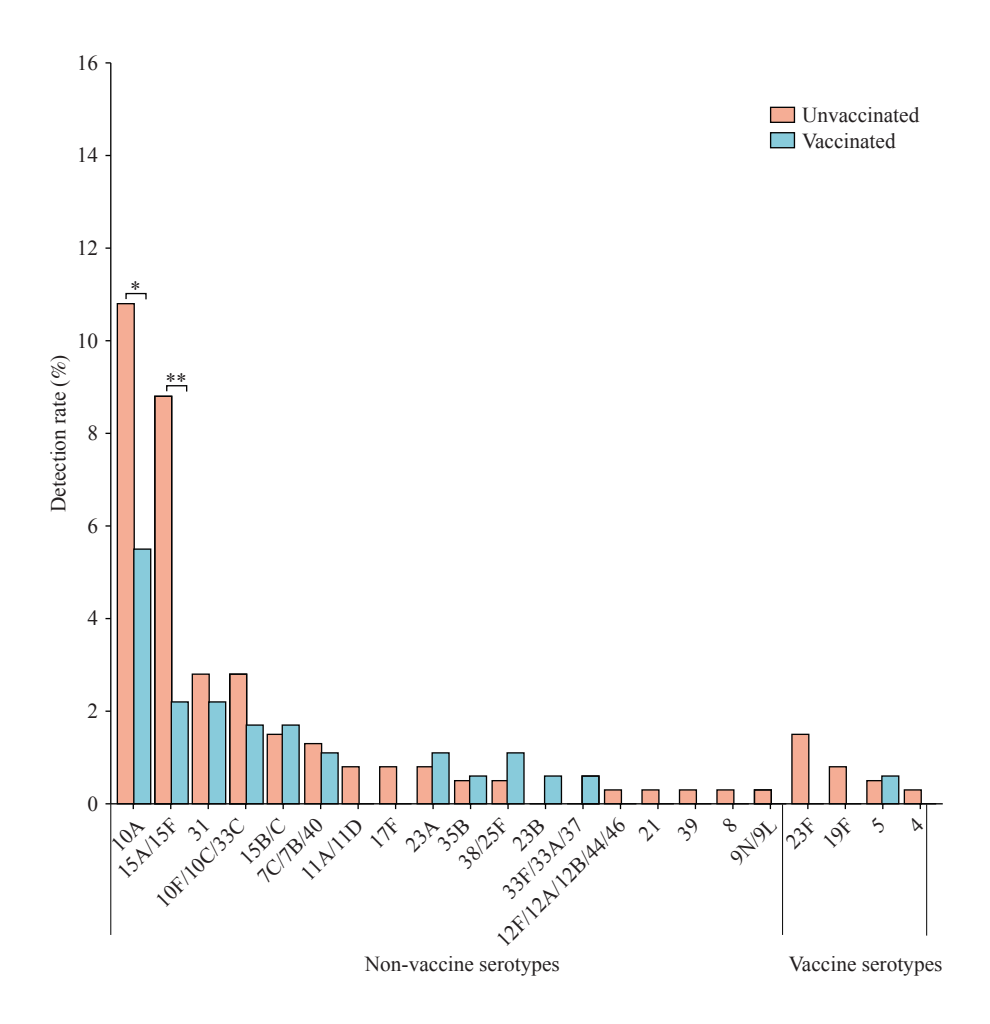


FIGURE 2. Detection rates of vaccine-type and non-vaccine serotypes during ARI episodes. Abbreviation: ARI=acute respiratory infection.

previously reported patterns. In Ulaanbaatar, Mongolia, a 44% reduction in vaccine-type carriage was observed following PCV13 vaccination, with serotypes 15A and 10A being the dominant serotypes (9). In Hong Kong, serogroup 15 has been reported to be the most frequently detected (10). Furthermore, a meta-analysis conducted between 2017 and 2024 identified 15A as the major non-vaccine serotype in Chinese children (11). Notably, the study reported 19F as the most prevalent serotype, which differed from our findings. This discrepancy may reflect differences in specimen types; the analysis included sterile site specimens and bronchoalveolar lavage fluid, which better represent serotypes causing clinical disease, whereas our study focused on ARI cases with mild symptoms, likely reflecting serotypes circulating within the community.

PCV immunization reduces the individual carriage of vaccine-type *S. pneumoniae*, thereby diminishing the transmission of these serotypes within the community (*12*). Although serotype replacement occurs frequently,

these emerging serotypes generally exhibit a lower invasive potential, resulting in a net benefit from vaccination with important public health implications. Long-term monitoring remains essential to determine whether vaccine-driven reductions in invasive pneumococcal persist and whether the invasive potential of non-vaccine serotypes remains stable or evolves as vaccine coverage expands.

The study had some limitations. First, although we evaluated the overall impact of PCV13 on pneumococcal detection, the small number of vaccine-type cases limited comprehensive subgroup analyses. Second, a substantial proportion of samples (32.8%) could not be serotyped, likely because of methodological factors. Multiplex PCR requires adequate template DNA, which makes low-load samples identified by tNGS more prone to serotyping failure. Moreover, some untypeable samples may have resulted from the limited serotype coverage of the PCR primers. Finally, our study was conducted exclusively in Eastern China, and given the regional variations in

TABLE 3. Cumulative incidence and risk ratios of pneumococcal detection during ARI episodes by PCV13 vaccination status in the original and IPTW cohorts.

Pneumococcal	PCV13 vaccination	n/N (%)	Cumulative incidenc	e Unadjusted <i>RR</i>	P	Adjusted RR	P
type	status		(%, 95% CI)	(95% CI)	(unadjusted)	(95% CI)*	(adjusted)
Original cohort							
All pneumococci	Unvaccinated	160/398 (40.2)	40.2 (35.3, 45.2)	Reference	-	Reference	-
	1–2 doses	11/38 (28.9)	28.9 (15.4, 45.9)	0.74 (0.44, 1.23)	0.260	0.80 (0.49, 1.32)	0.392
	3-4 doses	33/143 (23.1)	23.1 (16.4, 30.9)	0.57 (0.41, 0.78)	0.001	0.70 (0.50, 0.98)	0.036
Vaccine serotypes	Unvaccinated	12/398 (3.0)	3.0 (1.6, 5.2)	Reference	-	Reference	-
	≥1 dose	1/181 (0.6)	0.6 (0.0, 3.0)	0.18 (0.02, 1.36)	0.096	0.29 (0.04, 2.39)	0.251
Non-vaccine serotypes	Unvaccinated	99/398 (24.9)	24.9 (20.7, 29.4)	Reference	-	Reference	-
	1–2 doses	7/38 (18.4)	18.4 (7.7, 34.3)	0.75 (0.38, 1.48)	0.408	0.78 (0.41, 1.49)	0.454
	3-4 doses	18/143 (12.6)	12.6 (7.6, 19.2)	0.50 (0.31, 0.79)	0.003	0.61 (0.38, 0.97)	0.037
IPTW cohort [†]							
All pneumococci	Unvaccinated	222/578 (38.4)	38.4 (33.5, 43.3)	Reference	-	-	-
	1–2 doses	152/530 (28.7)	28.7 (13.3, 44.0)	0.75 (0.43, 1.30)	0.299	-	-
	3-4 doses	124/573 (21.6)	21.6 (13.9, 29.2)	0.56 (0.39, 0.82)	0.003	-	-
Non-vaccine serotypes	Unvaccinated	138/578 (23.9)	23.9 (19.7, 28.2)	Reference	-	-	-
	1–2 doses	82/530 (15.5)	15.5 (4.4, 26.6)	0.65 (0.31, 1.35)	0.247	-	-
	3-4 doses	52/573 (9.3)	9.1 (4.8, 13.5)	0.38 (0.23, 0.64)	<0.001	-	-

Note: Data are presented as n/N (%) unless otherwise specified.

Abbreviation: ARI=acute respiratory infection; PCV13=13-valent pneumococcal conjugate vaccine; *RR*=risk ratio; *CI*=confidence interval; IPTW=inverse probability of treatment weighting.

As there were no cases in the 1–2 dose group and only one case in the 3–4 dose group, the two groups were combined for analysis.

epidemiological patterns and transmission dynamics, our findings may not be fully generalizable to ARI populations in other geographic regions.

In conclusion, PCV13 vaccination reduced pneumococcal detection in children with ARI, highlighting the importance of complete early immunization. As serotype shifts occur, continuous surveillance is essential for guiding strategic adjustments and evidence-based control policies.

Conflicts of interest: No conflicts of interest.

Ethical statement: The Scientific Review Committee of Jiangsu Provincial Center for Disease Control and Prevention approved the study protocol (approval number: JSJK2022-B014-02).

Funding: Supported by Science Fund for Distinguished Young Scholars of Jiangsu Province (grant number: BK20220064).

doi: 10.46234/ccdcw2025.222

Copyright © 2025 by Chinese Center for Disease Control and Prevention. All content is distributed under a Creative Commons Attribution Non Commercial License 4.0 (CC BY-NC).

Submitted: August 04, 2025 Accepted: September 25, 2025 Issued: October 17, 2025

REFERENCES

- 1. Weiser JN, Ferreira DM, Paton JC. *Streptococcus pneumoniae*: transmission, colonization and invasion. Nat Rev Microbiol 2018;16 (6):355 67. https://doi.org/10.1038/s41579-018-0001-8.
- 2. Daningrat WOD, Amalia H, Ayu IM, Satzke C, Safari D. Carriage of

^{*} Adjusted for sex, disease history, mode of delivery, maternal age at delivery, maternal education level, maternal monthly income, number of household members, presence of children under 18 years old in the household, monthly household income, and baseline S. pneumoniae carriage.

[†] Weighted analysis was performed using IPTW estimated from multinomial logistic regression. The weighted results for vaccine serotypes were not estimated because of the small number of events. For the IPTW cohort, *n/N* values represent the sum of the IPTW weights and not the actual sample size.

^{*} Corresponding authors: Lunbiao Cui, lbcui@jscdc.cn; Jingxin Li, Lijingxin@jscdc.cn.

¹ School of Public Health, Southeast University, Nanjing City, Jiangsu Province, China; ² School of Public Health, National Vaccine Innovation Platform, Nanjing Medical University, Nanjing City, Jiangsu Province, China; ³ Jiangsu Provincial Medical Innovation Center, National Health Commission Key Laboratory of Enteric Pathogenic Microbiology, Jiangsu Provincial Center for Disease Control and Prevention (Jiangsu Provincial Academy of Preventive Medicine), Nanjing City, Jiangsu Province, China; ⁴ CanSino Biologics Inc., Tianjin, China.

[&]amp; Joint first authors.

China CDC Weekly

- Streptococcus pneumoniae in children under five years of age prior to pneumococcal vaccine introduction in Southeast Asia: a systematic review and meta-analysis (2001-2019). J Microbiol Immunol Infect 2022;55(1):6 17. https://doi.org/10.1016/j.jmii.2021.08.002.
- China National Clinical Research Center for Respiratory Diseases, National Center for Children's Health, Group of Respiralogy Chinese Pediatric Society, Chinese Medical Association, Chinese Medical Doctor Association Committee on Respiralogy Pediatrics, China Medicine Education Association Committee on Pediatrics, Chinese Research Hospital Association Committee on Pediatrics, et al. Chinese experts' consensus statement on diagnosis, treatment, and prevention of pneumococcal diseases in children. Chin J Appl Clin Pediatr 2020;35 (7):485 – 505. https://doi.org/10.3760/cma.j.cn101070-20200306-00329.
- 4. Li YQ, Wei MW, Cui LB, Huo X, Ma LS, Tao R, et al. Respiratory pathogens in infants and young children with acute respiratory illness: a prospective cohort study, China, 2023-2024. Front Public Health 2025;13:1548190. https://doi.org/10.3389/fpubh.2025.1548190.
- Wang J, Qiu L, Bai S, Zhao W, Zhang A, Li J, et al. Prevalence and serotype distribution of nasopharyngeal carriage of *Streptococcus* pneumoniae among healthy children under 5 years of age in Hainan Province, China. Infect Dis Poverty 2024;13(1):7. https://doi.org/10. 1186/s40249-024-01175-7.
- Wang L, Fu JJ, Liang ZX, Chen JC. Prevalence and serotype distribution of nasopharyngeal carriage of *Streptococcus pneumoniae* in China: a meta-analysis. BMC Infect Dis 2017;17(1):765. https://doi. org/10.1186/s12879-017-2816-8.
- Mika M, Maurer J, Korten I, Allemann A, Aebi S, Brugger SD, et al. Influence of the pneumococcal conjugate vaccines on the temporal variation of pneumococcal carriage and the nasal microbiota in healthy

- infants: a longitudinal analysis of a case-control study. Microbiome 2017;5(1):85. https://doi.org/10.1186/s40168-017-0302-6.
- van Gils EJM, Hak E, Veenhoven RH, Rodenburg GD, Bogaert D, Bruin JP, et al. Effect of seven-valent pneumococcal conjugate vaccine on *Staphylococcus aureus* colonisation in a randomised controlled trial. PLoS One 2011;6(6):e20229. https://doi.org/10.1371/journal.pone. 0020229.
- von Mollendorf C, Mungun T, Ulziibayar M, Nguyen CD, Batsaikhan P, Suuri B, et al. Effect of pneumococcal conjugate vaccination on pneumococcal carriage in hospitalised children aged 2-59 months in Mongolia: an active pneumonia surveillance programme. Lancet Microbe 2024;5(12):100929. https://doi.org/10.1016/S2666-5247(24) 00171-X.
- Chan KCC, Subramanian R, Chong P, Nelson EAS, Lam HS, Li AM, et al. Pneumococcal carriage in young children after introduction of PCV13 in Hong Kong. Vaccine 2016;34(33):3867 – 74. https://doi. org/10.1016/j.vaccine.2016.05.047.
- 11. Li Y, Wang SJ, Hong L, Xin LJ, Wang F, Zhou YB. Serotype distribution and antimicrobial resistance of *Streptococcus pneumoniae* in China among children under 14 years of age post-implementation of the PCV13: a systematic review and meta-analysis (2017-2024). Pneumonia (Nathan) 2024;16(1):18. https://doi.org/10.1186/s41479-024-00141-z.
- 12. Chan J, Mungun T, Batsaixan P, Ulziibayar M, Suuri B, Otgonbayar D, et al. Direct and indirect effects of 13-valent pneumococcal conjugate vaccine on pneumococcal carriage in children hospitalised with pneumonia from formal and informal settlements in Mongolia: an observational study. Lancet Reg Health West Pac 2021;15:100231. https://doi.org/10.1016/j.lanwpc.2021.100231.

SUPPLEMENTARY MATERIAL

The targeted next-generation sequencing (tNGS) assay was performed following standardized procedures, including nucleic acid extraction and library preparation.

Nucleic Acid Extraction

From each pharyngeal swab sample, 1.3~mL of specimen was aliquoted and mixed with $13~\mu\text{L}$ of exogenous internal control RNA, followed by centrifugation. The resulting pellet was collected, and nucleic acids were extracted using a commercial nucleic acid extraction kit (KS118-BYTQ, Guangzhou, China) according to the manufacturer's instructions.

Library Preparation and Sequencing

An appropriate volume of nucleic acid was transferred into a 96-well plate, with 2 μ L of synthesis primers and synthesis buffer added to each well, for a final reaction volume of 20 μ L. First-strand cDNA synthesis was performed under the following conditions: incubation at 25 °C for 5 min, reaction at 37 °C for 45 min, denaturation at 85 °C for 5 s, and maintenance at 4 °C. The cDNA products were then subjected to multiplex PCR for target enrichment using a reaction mixture containing multiplex PCR premix and 11 μ L of cDNA template. The amplification program was as follows: 95 °C for 3 min, followed by 30 cycles of 95 °C for 30 s, 60 °C for 30 s, and 72 °C for 30 s, with a final extension at 72 °C for 1 min. PCR products were purified using magnetic beads, airdried at room temperature, and eluted in 13.5 μ L RNase-free water.

For library amplification, 11.5 μ L of purified product was added to the library amplification premix. Following PCR amplification and a second round of magnetic bead purification, libraries were eluted in 20 μ L. Library concentration was quantified using a Qubit fluorometer. Qualified libraries showed a distinct peak within the 250–350 bp range, and libraries lacking a peak or with <20% representation were considered failed. Qualified libraries were pooled in equimolar amounts, purified with magnetic beads, and assessed for fragment size distribution using a Qsep100 nucleic acid analyzer. The pooled library was diluted to 1 pmol/L, denatured with NaOH, and loaded onto the MiniSeqDx-CN sequencing platform.

Bioinformatics Analysis

Raw sequencing data were analyzed using the Proprietary Pathogen Data Analysis Management System (KingCreate, Guangzhou, China). Quality control was performed, and only datasets meeting the following criteria were included: sequencing quality score $Q30 \ge 75\%$ and a minimum of 50,000 raw reads per sample. High-quality reads were subsequently aligned to a reference database, and normalized read counts were applied to determine pathogen positivity. A pathogen was considered positive if at least one specific target region produced a normalized read count ≥ 10.5 ; otherwise, it was classified as negative.

SUPPLEMENTARY TABLE S1. Baseline demographic characteristics of the participants at the recruitment.

Characteristics	Participants included in the analysis (<i>N</i> =579)	All enrolled children (N=796)	Р
Infant sex, n (%)			0.910
Female	269 (46.5)	373 (46.9)	
Male	310 (53.5)	422 (53.1)	
Infant age, median (IQR), days	71.0 (66.0, 78.0)	71.0 (66.0, 77.3)	0.757
Infant height, median (IQR), cm	60.0 (59.0, 62.0)	60.0 (59.0, 62.0)	0.073
Infant weight, median (IQR), kg	6.3 (5.8, 6.8)	6.3 (5.8, 6.8)	0.585
Infant birth length, median (IQR), cm	50.0 (50.0, 50.0)	50.0 (50.0, 50.0)	0.113
Infant birth weight, median (IQR), kg	3.4 (3.2, 3.7)	3.4 (3.2, 3.7)	0.346
Infant disease history*, n (%)			0.831
Yes	18 (3.1)	22 (2.8)	
No	561 (96.9)	774 (97.2)	

Continued

Characteristics	Participants included in the analysis (<i>N</i> =579)	All enrolled children (N=796)	P
Maternal mode of delivery, <i>n</i> (%)			>0.999
Full-term vaginal delivery	291 (50.3)	399 (50.1)	
Cesarean delivery	288 (49.7)	397 (49.9)	
Maternal feeding pattern, n (%)			0.415
Breastfeeding	523 (90.3)	701 (88.1)	
Not breastfeeding after birth	47 (8.1)	80 (10.1)	
Mixed feeding	9 (1.6)	15 (1.9)	
Maternal age, n (%), years			0.822
<35	503 (86.9)	687 (86.3)	
≥35	76 (13.1)	109 (13.7)	
Maternal education, n (%)			0.854
Middle school or below	162 (28.0)	210 (26.4)	
High school or vocational school	100 (17.3)	141 (17.7)	
Junior college	152 (26.3)	223 (28.0)	
Bachelor degree or above	165 (28.5)	222 (27.9)	
Maternal monthly income, n (%), CNY			0.800
<1,000	245 (42.3)	329 (41.3)	
1,000–6,999	270 (46.6)	370 (46.5)	
≥7,000	64 (11.1)	97 (12.2)	
No. of household members, n (%)			0.835
≤4	421 (72.7)	584 (73.4)	
>4	158 (27.3)	212 (26.6)	
With household members <18 years of age, n (%)			0.513
Yes	329 (56.8)	437 (54.9)	
No	250 (43.2)	359 (45.1)	
Monthly household income, n (%), CNY			0.904
<10,000	175 (30.2)	237 (29.8)	
≥10,000	404 (69.8)	559 (70.2)	
Baseline S. pneumoniae carriage			>0.999
Yes	21 (3.6)	29 (3.6)	
No	553 (95.5)	761 (95.6)	
Missing	5 (0.9)	6 (0.8)	
Received first dose of PCV13 before enrollment, n (%)			0.781
Yes	54 (9.3)	79 (9.9)	
No	525 (90.7)	717 (90.1)	

Abbreviation: PCV13=13-valent pneumococcal conjugate vaccine; CNY=Chinese Yuan; COVID-19=coronavirus disease 2019.

^{*} Infant disease history includes pneumonia, jaundice, COVID-19, and lactose intolerance.

Preplanned Studies

Protective Effect and Immune Mechanism of EPCP009 Booster Immunization after BCG Prime Immunization Against Tuberculosis in Mice — China, 2024

Ruihuan Wang¹; Xueting Fan¹; Machao Lii¹; Xiuqin Zhao¹; Xinyue He¹; Kanglin Wan¹; Haican Liu^{1,#}

Summary

What is already known about this topic?

At present, relatively few theoretical studies exist on the immunization strategies of tuberculosis vaccines, especially regarding the types of subunit protein vaccines suitable for combined application with Bacillus Calmette–Guérin (BCG).

What is added by this report?

The study demonstrated that EPCP009, a novel subunit vaccine candidate, maintains BCG colonization in murine spleens while enhancing protection. Notably, a single dose of EPCP009 combined with BCG was superior to multiple doses in terms of both short-term (6-week) and long-term (12-week) protection.

What are the implications for public health practice?

These studies provide a theoretical basis for enhancing the immune strategy of tuberculosis vaccines and contribute to the development of combined BCG and subunit protein vaccines.

ABSTRACT

Introduction: Bacillus Calmette–Guérin (BCG) is the only approved tuberculosis (TB) vaccine; however, it has partial efficacy and time-limited protection. Subunit booster vaccines may enhance the effects of BCG; however, their efficacy depends on their composition.

Methods: Six-week-old BALB/c mice received primary immunization with BCG, followed by EPCP009 protein boosters (mixed with DDA/poly:IC [DP] adjuvant) once, twice, or thrice (2-week intervals). Six weeks after the first immunization, blood and spleen samples were collected. Levels of antibodies and cytokines were assessed via enzyme-linked immunosorbent assay (ELISA), Luminex, and enzyme-linked immunospot (ELISpot) The ability of splenocytes to inhibit *Mycobacterium tuberculosis* (Mtb) was assessed by MGIA, and pathological analyses were

conducted on the liver, spleen, and lung. In addition, mice were immunized with EPCP009 or H4 protein separately. BCG was administered intravenously 6 weeks later, and spleens were collected at 3.5 weeks to quantify the BCG bacterial load.

Results: BCG combined with a single EPCP009 dose provided better short-term (6-week) and long-term (12-week) protection than multiple doses. During the long-term process, the levels of purified protein derivative (PPD)-specific interferon (IFN)- γ and granulocyte-macrophage colony-stimulating factor (GM-CSF) remained relatively high. No significant differences in the BCG colony counts were observed among the EPCP009/DP, phosphate-buffered saline (PBS), and DP groups.

Conclusions: These findings demonstrate that BCG vaccination combined with a single dose of EPCP009 enhances protective efficacy against TB. This study provides a critical theoretical basis for designing booster immunization strategies for TB vaccines.

Tuberculosis (TB) is the second leading cause of death from a single infectious agent, following coronavirus disease 2019 (COVID-19) (1). According to the World Health Organization (WHO) Global TB Report 2023, more than 10.6 million individuals, with approximately 90% of them adults, contracted TB by 2022 (2). A quarter of the world's population is estimated to be infected with *Mycobacterium tuberculosis* (Mtb). The COVID-19 pandemic has reduced healthcare accessibility for patients with TB, setting back global TB prevention and control efforts (3). Developing new TB vaccine strategies is essential for achieving the ambitious goal of ending TB by 2030.

Mycobacterium bovis Bacillus Calmette-Guérin (BCG) is the only approved preventive vaccine offering protection against severe TB for young children. However, its efficacy in adults remains unclear. The

WHO does not recommend BCG revaccination in adults because of insufficient evidence supporting its effectiveness (4). Numerous TB vaccines are currently under development, with 18 undergoing clinical trials worldwide. Among these, the subunit TB vaccine M72/AS01_E has demonstrated 49.7% efficacy [90% confidence interval (CI), 12.1, 71.2] against active pulmonary TB in adults; however, its efficacy requires further evaluation (5). Clinical trials of the H4:IC31 and M72/AS01_F adjuvant protein subunit vaccines coadministered with BCG show promising results and offer prospects for different immunization strategies. Viral vector and mRNA vaccines have received special attention as emerging platforms. The ChAdOx1 85A viral vector vaccine induced Ag85-specific CD4+T and CD8⁺T cells and was well tolerated and immunogenic in a phase I clinical trial (6). Animal models have demonstrated both preventive and therapeutic effects of mRNA vaccines in zebrafish. However, the clinical protective effect of the existing single-dose virus vector vaccine is not ideal, and the mRNA vaccine still faces challenges, such as stability.

Unlike attenuated or live vaccines, subunit protein vaccines have clear antigenic components and high safety profiles, making them particularly suitable for HIV-infected and immunocompromised populations. However, subunit vaccines often require multiple booster doses to maximize efficacy, posing challenges TB-endemic regions with limited resources. Heterologous prime-boost regimens using BCG and different antigen-expressing vectors can induce more robust T-cell and humoral responses (7). With global BCG coverage reaching 90%, new TB vaccine development focuses on designing booster vaccines following initial BCG immunization. Most TB subunit vaccines in clinical trials, such as H4/IC31 and H56/IC31, are efficacious when used as boosters after BCG vaccination (8–9). However, no approved immune-enhancing vaccines are currently available for use with BCG; the reasons remain unclear. Most subunit vaccines share some or all antigenic components with BCG, which may inhibit BCG growth and immune responses.

As part of our TB vaccine development program, we designed the EPCP009 fusion protein, which is composed of four antigens that are either not expressed or expressed at low levels in BCG. This design broadens the range of immune protection without interfering with BCG-mediated immune responses. We previously demonstrated superior effectiveness of BCG prime-EPCP009 booster regimen over the

rBCG-EPCP009 regimen (10). Herein, BALB/c mice were used to investigate the immunogenicity, efficacy, and safety of BCG in combination with single, double, and triple doses of EPCP009/dimethyl-dioctyldecylammonium bromide/polyinosinic-polycytidylic acid (DDA/poly:IC). In addition, we assessed whether EPCP009 inhibited BCG growth, elucidating its potential as a BCG booster vaccine.

Mycobacterium bovis BCG-China and Mycobacterium tuberculosis H37Rv (ATCC27294) strains were maintained at −80 °C and cultured on Difco™ Middlebrook 7H9/7H10 agar (BD, USA) supplemented with 10% OADC, 0.5% glycerol, and 0.05% tween 80. Recombinant pET28a(+) plasmid expressing H4 antigen (TB10.4-Ag85B fusion protein) was constructed in our laboratory and transformed into Escherichia coli DH5 α /BL21(DE3).

Female BALB/c mice (6 weeks old, specific-pathogen-free) were purchased from Beijing HFK Bioscience Co., Ltd. (Beijing, China). Mice were acclimatized for 5 days in pathogen-free cages before random allocation to five groups (*n*=12/group).

Each vaccine dose containing 10 μg of EPCP009 protein was formulated in phosphate-buffered saline (PBS) (pH 7.4) with 250 μg of DDA/50 μg of poly:IC adjuvant. BCG-China [1×10⁶ colony-forming units (CFU)] or EPCP009 formulations were administered intradermally (100 μL) or subcutaneously (200 μL), respectively. Booster immunizations with EPCP009 were administered at 2-week intervals after BCG priming (BCG+1×, BCG+2×, or BCG+3×EPCP009 groups) (11). The control group received the DDA/poly:IC (Sigma, Germany) adjuvant or PBS alone (Figure 1).

Spleens were harvested at 6/12 weeks postimmunization, minced through 70-µm strainers (BD, USA), and centrifuged (800 ×g, 30 min). The cells were washed twice with RPMI 1640 (Gibco, USA), resuspended in 10% fetal bovine serum-RPMI, and adjusted to 2×10^5 cells/well (ELISpot/Luminex) or 5×10^6 cells/well (MGIA).

ELISpot: Splenocytes $(2\times10^5/\text{well})$ were stimulated with 2 µg of PPD for 20 h (37 °C, 5% CO₂) and detected using the ELISpot assay kit (Dakewe, China) (12).

Luminex: Supernatants from PPD-stimulated splenocytes (10 µg/well, 24 h) were analyzed for nine cytokines (interferon [IFN]- γ , interleukin [IL]-2, tumor necrosis factor [TNF]- α , IL-17, granulocytemacrophage colony-stimulating factor (GM-CSF), IL-12, IL-4, IL-6, IL-10) using the magnetic bead assay

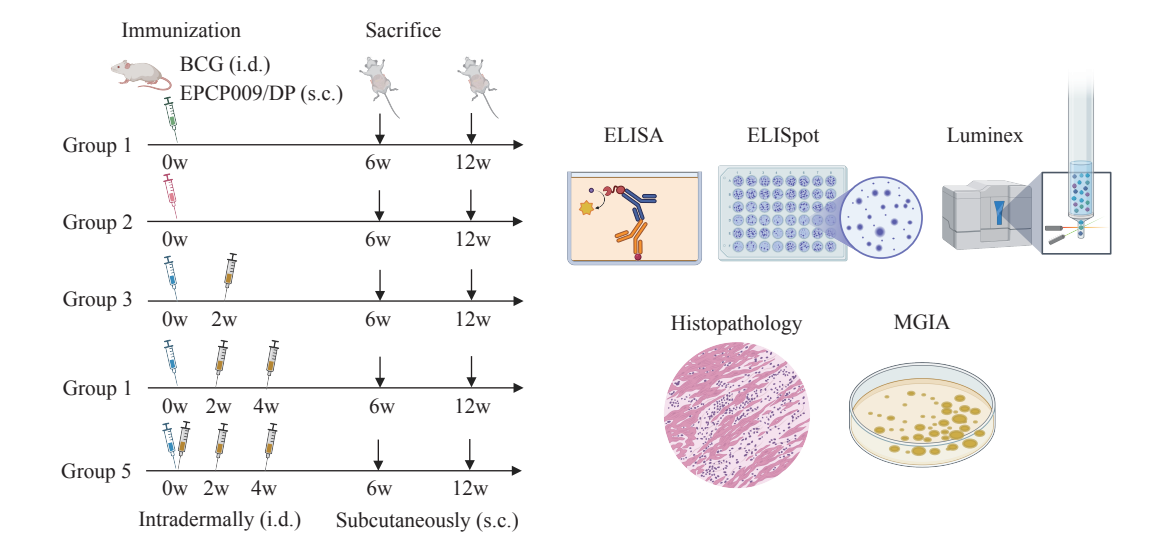


FIGURE 1. Vaccination and testing regimen schedules. Abbreviation: ELISA=enzyme-linked immunosorbent assay; ELISPOT=enzyme-linked immunospot; MGIA=mycobacterial growth inhibition assay.

(R&D Systems, USA).

Enzyme-linked immunosorbent assay (ELISA): A 96-well ELISA plate was coated with 200 ng of EPCP009 antigen, horseradish peroxidase-labeled goat anti-mouse IgG was used as the secondary antibody, and 3,3′,5,5′-tetramethylbenzidine substrate was added to develop color.

Spleen, liver, and lung tissues collected at 6 weeks of age were fixed in 4% paraformaldehyde for hematoxylin and eosin (H&E) staining (Beijing Kaike Green Technology Co., Ltd., China).

Splenocytes (5×10^6 cells) were co-cultured with Mtb H37Rv (50 CFU) for 72 h at 37 °C and 5% CO₂. After incubation, the supernatant was removed by centrifugation at 4,000 rpm for 10 min. The cells were lysed by adding 500 μ L of pre-cooled sterile water in an ice bath per well to release intracellular bacteria, and 50 μ L was spread on the 7H10 medium containing 10% OADC. Six replicates were set up for each sample.

The H4 protein (containing the Mtb/BCG-shared antigens TB10.4 and Ag85B) served as a positive control in assessing cross-immunogenicity between EPCP009 and BCG (8). Recombinant EPCP009 and H4 were expressed in *E. coli* BL21(DE3) cells using pET28a(+) vectors with kanamycin selection (25 µg/mL). Protein induction was performed with 1 mmol/L of IPTG (Sigma, Germany) for 4.5 h at 37 °C, followed by nickel-affinity chromatography purification (GE Healthcare, USA) from inclusion bodies.

Mice were divided into four groups: PBS,

DDA/poly:IC (DP) adjuvant (250 µg DDA/50 µg poly:IC), EPCP009/DP (10 µg protein + adjuvant), and H4/DP (10 µg protein + adjuvant). Immunization was administered subcutaneously at 0-, 2-, and 4-week intervals. Six weeks after immunization, BCG-China (1×10⁷ CFU) was administered intravenously. The spleens were collected at 3.5 weeks, lysed, and the BCG bacterial load was quantified using 7H10 medium.

Data are presented as mean ± standard deviation (GraphPad Prism 8.0, San Diego, California, USA, www.graphpad.com). Group comparisons were performed using one-way analysis of variance (ANOVA) with Tukey's multiple comparison test.

The amounts of IFN- γ (A,C) and IL-4 (B,D) secreted by mouse splenic lymphocytes at 6 and 12 weeks were determined using the ELISpot assay.

Six and 12 weeks after the initial immunization, mouse splenic lymphocytes were stimulated with PPD (Figure 2). All vaccine groups produced higher levels of the protective cytokine IFN- γ at both 6 (P<0.05) and 12 (P<0.05) weeks than the PBS group. The BCG+1×EPCP009 group induced higher IFN-γ production than the **BCG** (P < 0.001)BCG+2×EPCP009 (P<0.05) groups at both time group induced The BCG+1×EPCP009 comparable production of IFN- γ to BCG+3×EPCP009 group at 6 weeks (P=0.041), and significantly higher than the BCG+3×EPCP009 group at 12 weeks (P<0.001). IL-4 levels in the BCG+1×EPCP009 group were significantly higher than those in the PBS (P<0.001) and BCG (P<0.001)

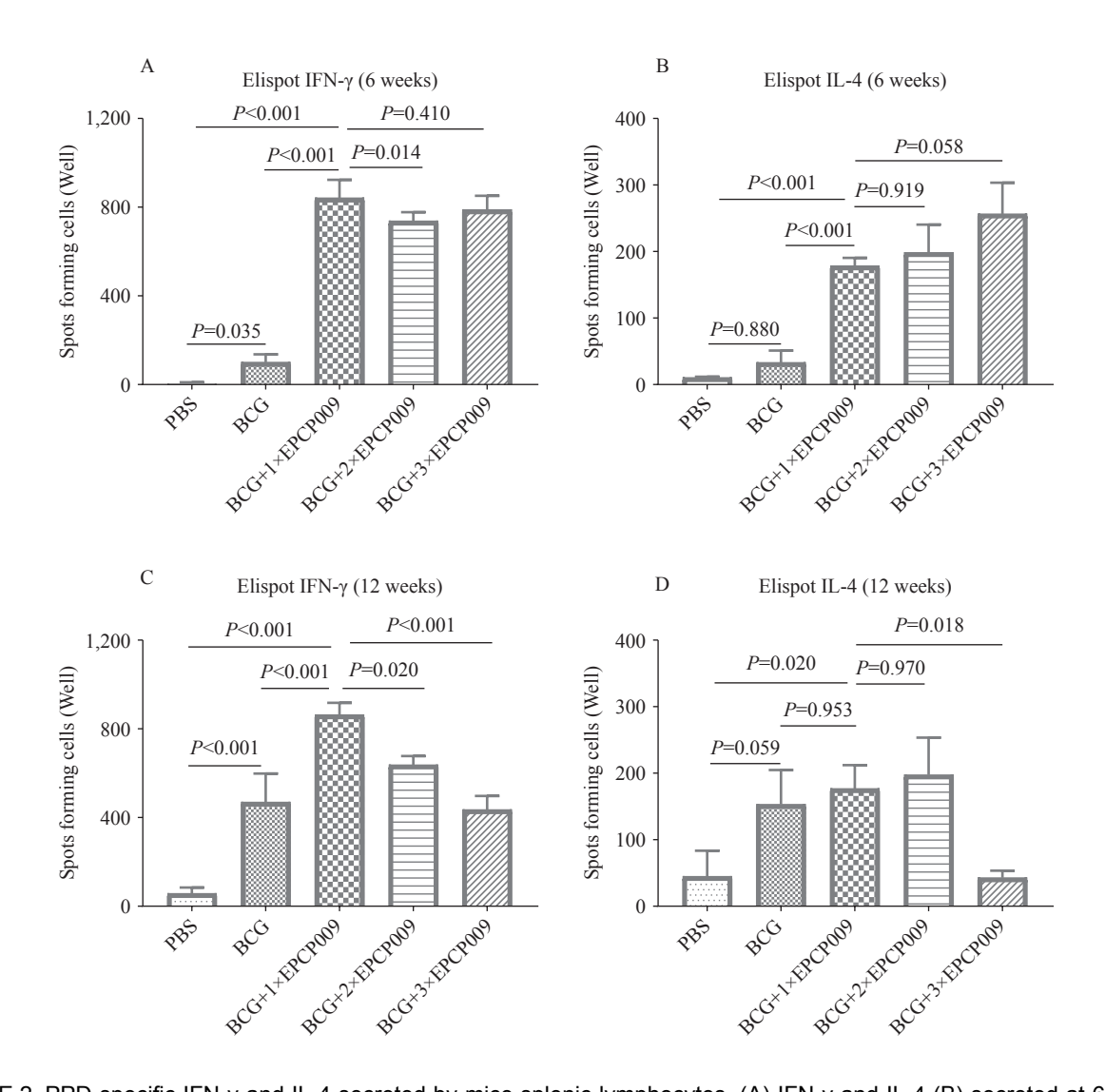


FIGURE 2. PPD-specific IFN-γ and IL-4 secreted by mice splenic lymphocytes. (A) IFN-γ and IL-4 (B) secreted at 6 weeks; (C) IFN-γ and IL-4 (D) secreted at 12 weeks. Abbreviation: PPD=purified protein derivative; ELISpot=enzyme-linked immunospot.

groups at 6 weeks, but comparable to those in the BCG+2×EPCP009 (P=0.919) and BCG+3×EPCP009 (P=0.058) groups. IL-4 levels in the BCG+1×EPCP009 group were comparable to those in the BCG (P=0.953) and BCG+2×EPCP009 (P=0.970) groups at 12 weeks but were significantly higher than those in the BCG+3×EPCP009 group (P=0.018).

Six weeks post-immunization, mouse splenic lymphocytes were stimulated with PPD (Figure 3 and Supplementary Figure S1, available at https://weekly.chinacdc.cn/). The BCG+1×EPCP009 group produced higher levels of IFN- γ , IL-2, TNF- α , IL-17, GM-CSF, IL-12, IL-4, IL-6, and IL-10 than the PBS and BCG groups (both P<0.05). In addition, the BCG+1×EPCP009 group induced higher levels of IFN- γ , IL-2, IL-12, IL-17, and GM-CSF than the BCG+2×EPCP009 group (P<0.05). Compared with

the BCG+3×EPCP009 group, the BCG+1×EPCP009 group had significantly higher IL-2 levels (*P*<0.001) but lower IL-6 levels (*P*<0.001).

At 12 weeks post-immunization, the BCG+1× EPCP009 group induced higher levels of IFN- γ , GM-CSF, and IL-4 than the PBS, BCG, BCG+2×EPCP009, and BCG+3×EPCP009 groups (P<0.05) (Figure 3 and Supplementary Figure S1). Furthermore, the BCG+1×EPCP009 group produced higher levels of IL-17 than the BCG+2×EPCP009 and BCG+3×EPCP009 groups (P<0.05).

The ability and duration of immune-mediated inhibition of Mtb growth *in vitro* were evaluated, for which splenocytes were isolated from immunized mice and co-cultured with H37Rv at 6 and 12 weeks following initial immunization. The bacterial colonies were quantified and expressed as log10 colony-forming

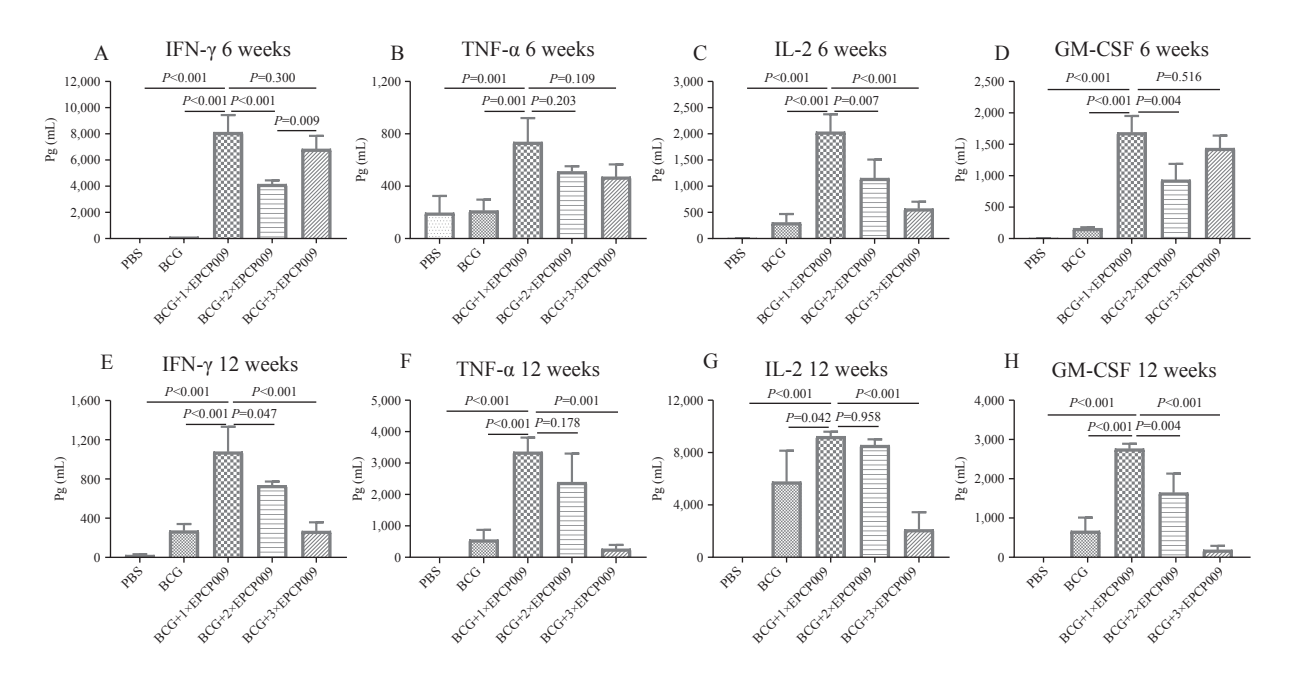


FIGURE 3. Levels of cytokines secreted by PPD-stimulated spleen lymphocytes in mice 6 and 12 weeks from initial immunization. (A) IFN- γ , (B) TNF- α , (C) IL-2 and (D) GM-CSF secreted at 6 weeks; (E) IFN- γ , (F) TNF- α , (G) IL-2 and (H) GM-CSF secreted at 12 weeks.

units (lgCFUs) per sample. At 6 weeks postimmunization, the BCG+1×EPCP009 group displayed significantly lower colony counts than the PBS, BCG, and BCG+2×EPCP009 groups (*P*<0.05), and slightly lower colony counts than the BCG+3×EPCP009 group (*P*=0.063). At 12 weeks, the BCG+1×EPCP009 group had significantly lower colony counts than the other groups (*P*<0.001) (Figure 4).

At 6 weeks post-immunization, histological analysis of the liver, spleen, and lung tissues revealed no significant between-group differences. All organs exhibited normal morphology with no evidence of cellular edema or necrosis (Figure 5).

The H4/DP group demonstrated significantly fewer BCG colonies in the spleen than the PBS (P=0.005) and DP (P=0.004) groups, indicating cross-immunity between H4 and BCG (Figure 6). In contrast, the EPCP009/DP group displayed significant no difference in BCG colony counts compared to the PBS (P=0.967) and DP (P=0.986) groups, indicating that EPCP009 inhibit BCG did not growth colonization.

DISCUSSION

After decades of global efforts, more than a dozen TB vaccines have reached clinical trials, primarily falling into two categories: whole mycobacterium-derived vaccines (live attenuated and inactivated) and

subunit vaccines (13). Subunit vaccines, which are particularly promising BCG boosters, enhance and prolong BCG-induced immunity. Notably, subunit vaccines such as H4-IC31, Mtb72F/AS02A, and ID93/GLA-SE offer superior protection compared with BCG alone (14). A limited number of antigens can be selected for subunit vaccines; therefore, antigen selection and immunization frequencies are critical. EPCP009, introduced herein, was administered once after BCG vaccination to significantly improve immunization efficacy.

EPCP009 uniquely combines four antigens, CFP-10, ESAT-6, PPE18, and PstS1, none of which is expressed or minimally expressed in BCG. This broad antigen spectrum, including the highly immunogenic PstS1, which is not yet featured in clinical TB vaccines, enhances the immune response breadth (15). Unlike certain subunit vaccines that risk immune-mediated side effects due to antigens shared with BCG, EPCP009 avoids cross-reactivity, preserving BCG colonization and efficacy. Comparative studies with the H4 vaccine, which inhibits BCG growth, confirmed the absence of EPCP009 interference with BCG, highlighting its suitability as a BCG booster.

Given the intracellular nature of the Mtb, cellular immunity is paramount (16). EPCP009, in a single dose post-BCG, significantly elevated protective cytokines (IFN- γ , GM-CSF, and IL-2) at both 6 and 12 weeks, outperforming multiple-dose regimens and

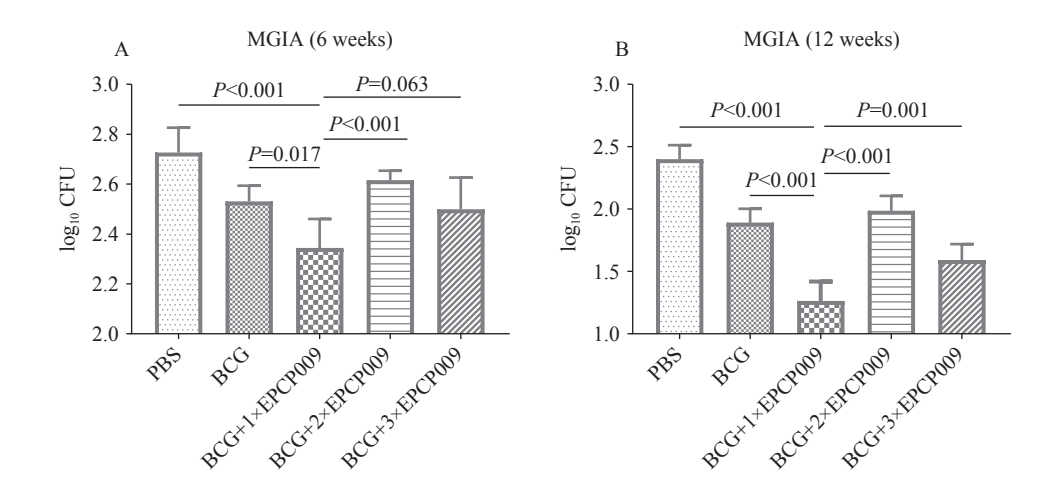


FIGURE 4. In vitro growth inhibition of Mtb H37Rv with splenocytes from immunized BALB/c mice at (A) 6 weeks and (B) 12 weeks.

Abbreviation: MGIA=mycobacterial growth inhibition assay.

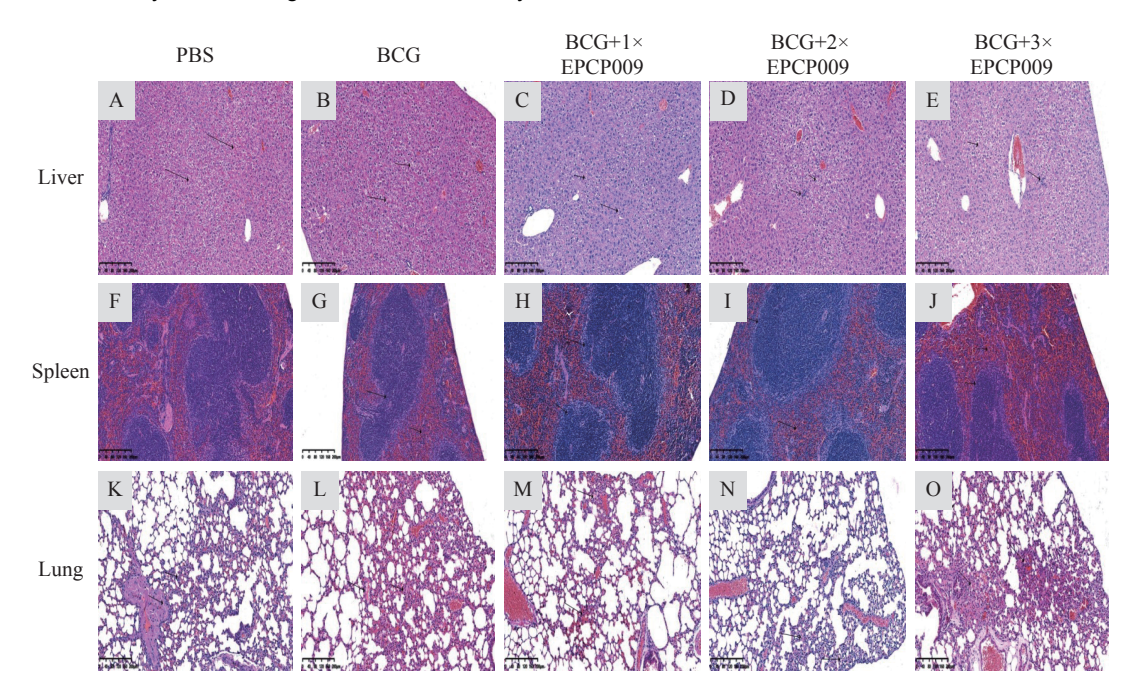


FIGURE 5. Safety analysis of BCG prime-EPCP009 booster with different number of immunizations. After 6 weeks of the last immunization, the liver (A, B, C, D, E), spleen (F, G, H, I, J), and lungs (K, L, M, N, O) of the PBS, BCG, BCG+1×EPCP009, BCG+2×EPCP009, BCG+3×EPCP009 groups were aseptically isolated and stained with H&E. Abbreviation: H&E=hematoxylin and eosin.

BCG alone. Thus, a durable Th1-biased immune response is crucial for Mtb control. Moreover, the MGIA assav revealed that a single booster immunization with EPCP009 after **BCG** immunization inhibited Mtb growth in vitro, and this inhibitory effect remained significant, especially after 12 weeks of immunization. The immunized groups produced higher antibody levels for longer durations (6 and 12 weeks) (Supplementary Figure S2, available at https://weekly.chinacdc.cn/). In addition, BCG

primary immunization with EPCP009 multiple booster immunization significantly decreased protective cytokines such as IFN- γ , TNF- α , IL-2, and GM-CSF, and other protective cytokines at week 12, with poor protection, which may be attributed to immune tolerance caused by multiple booster immunization. In conclusion, booster immunization with EPCP009 after BCG primary immunization has the potential for long-term protection.

Despite its promise, this study acknowledges its

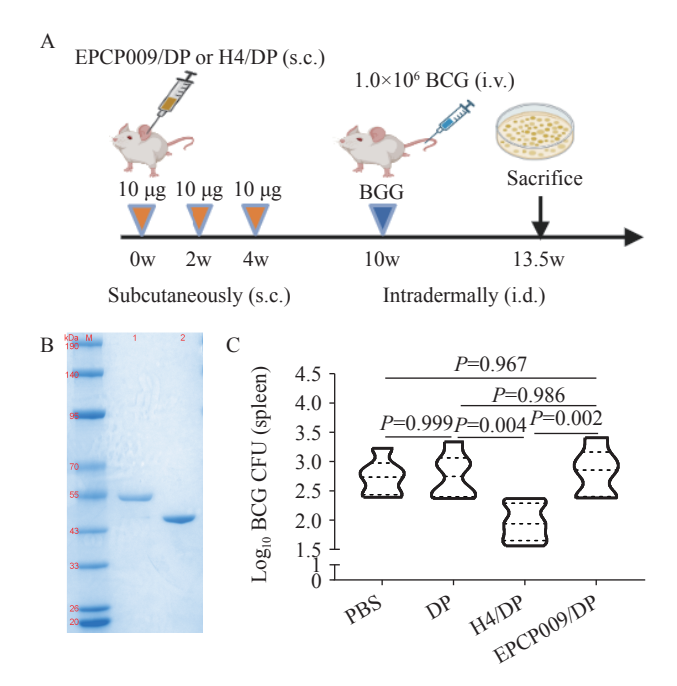


FIGURE 6. Verification of cross-immune responses between EPCP009 and H4 proteins and BCG. (A) Cross immunization schemes. (B) Protein expression of EPCP009 and H4. (C) The number of BCG colonies in the spleens of BCG-inoculated mice after immunization with PBS, DP, H4/DP and EPCP009/DP.

Note: For (B), lane M, molecular weight marker of the prestained protein; lane 1, purified EPCP009 protein, 51 kD; lane 2, purified H4 protein, 46 kD.

limitations, including the need for validation across different BCG strains and animal models to better predict clinical efficacy. Nonetheless, EPCP009's single-dose efficacy, both short- and long-term, makes it a highly promising candidate for an effective TB vaccine strategy, offering a significant advancement over current options.

Conflicts of interest: No conflicts of interest.

Ethical statements: All animal experiments were conducted in accordance with the animal welfare guidelines and approved by the Animal Experimental Ethical Committee of the Chinese Center for Disease Control and Prevention (2022-CCDC-IAC-026).

Funding: Supported by the Youth Fund for Enhancing the Capability of Infectious Disease Surveillance and Prevention (no. 102393240020020000003) and the Fourteenth Five-Year National Key Research and Development Program of China (no. 2023YFC2307201).

doi: 10.46234/ccdcw2025.225

Control and Prevention, Chinese Center for Disease Control and Prevention, Beijing, China.

Copyright © 2025 by Chinese Center for Disease Control and Prevention. All content is distributed under a Creative Commons Attribution Non Commercial License 4.0 (CC BY-NC).

Submitted: July 01, 2025 Accepted: September 30, 2025 Issued: October 17, 2025

REFERENCES

- 1. Rath S, Mishra B, Mohapatra PR, Datta A, Durgeshwar G, Vedala M, et al. Tuberculosis and COVID-19: An epidemic submerged in the pandemic: a case series and review of current literature. J Family Med Prim Care 2022;11(10):6576 80. https://doi.org/10.4103/jfmpc.ifmpc 258 22.
- Reid M, Agbassi YJP, Arinaminpathy N, Bercasio A, Bhargava A, Bhargava M, et al. Scientific advances and the end of tuberculosis: a report from the Lancet Commission on Tuberculosis. Lancet 2023;402 (10411):1473 – 98. https://doi.org/10.1016/S0140-6736(23)01379-X.
- Crisan-Dabija R, Grigorescu C, Pavel CA, Artene B, Popa IV, Cernomaz A, et al. Tuberculosis and COVID-19: lessons from the past viral outbreaks and possible future outcomes. Can Respir J 2020;2020: 1401053. https://doi.org/10.1155/2020/1401053.
- Schrager LK, Chandrasekaran P, Fritzell BH, Hatherill M, Lambert PH, McShane H, et al. WHO preferred product characteristics for new vaccines against tuberculosis. Lancet Infect Dis 2018;18(8):828 – 9. https://doi.org/10.1016/S1473-3099(18)30421-3.
- Ji ZH, Jian MM, Chen TG, Luo LS, Li LB, Dai XT, et al. Immunogenicity and safety of the M72/AS01_E candidate vaccine against tuberculosis: a meta-analysis. Front Immunol 2019;10:2089. https://doi.org/10.3389/fimmu.2019.02089.
- Wilkie M, Satti I, Minhinnick A, Harris S, Riste M, Ramon RL, et al. A
 phase I trial evaluating the safety and immunogenicity of a candidate
 tuberculosis vaccination regimen, ChAdOx1 85A prime MVA85A
 boost in healthy UK adults. Vaccine 2020;38(4):779 89. https://doi.
 org/10.1016/j.vaccine.2019.10.102.
- Wu YQ, Cai M, Ma JL, Teng XD, Tian MP, Bassuoney EBMB, et al. Heterologous boost following *Mycobacterium bovis BCG* reduces the late persistent, rather than the early stage of intranasal tuberculosis challenge infection. Front Immunol 2018;9:2439. https://doi.org/10.3389/ fimmu.2018.02439.
- Bekker LG, Dintwe O, Fiore-Gartland A, Middelkoop K, Hutter J, Williams A, et al. A phase 1b randomized study of the safety and immunological responses to vaccination with H4:IC31, H56:IC31, and BCG revaccination in *Mycobacterium tuberculosis*-uninfected adolescents in Cape Town, South Africa. EClinicalMedicine 2020;21:100313. https://doi.org/10.1016/j.eclinm.2020.100313.
- Dijkman K, Lindenstrøm T, Rosenkrands I, Søe R, Woodworth JS, Arlehamn CSL, et al. A protective, single-visit TB vaccination regimen by co-administration of a subunit vaccine with BCG. NPJ Vaccines 2023;8(1):66. https://doi.org/10.1038/s41541-023-00666-2.
- Wang RH, Fan XT, Xu D, Li MC, Zhao XQ, Cao B, et al. Comparison of the immunogenicity and efficacy of rBCG-EPCP009, BCG prime-EPCP009 Booster, and EPCP009 protein regimens as tuberculosis vaccine candidates. Vaccines (Basel) 2023;11(12):1738. https://doi.org/10.3390/vaccines11121738.
- Woodworth JS, Clemmensen HS, Battey H, Dijkman K, Lindenstrøm T, Laureano RS, et al. A *Mycobacterium tuberculosis*-specific subunit vaccine that provides synergistic immunity upon co-administration with Bacillus Calmette-Guérin. Nat Commun 2021;12(1):6658. https://doi. org/10.1038/s41467-021-26934-0.
- 12. Wang RH, Fan XT, Jiang Y, Li GL, Li MC, Zhao XQ, et al. Immunogenicity and efficacy analyses of EPC002, ECA006, and EPCP009 protein subunit combinations as tuberculosis vaccine

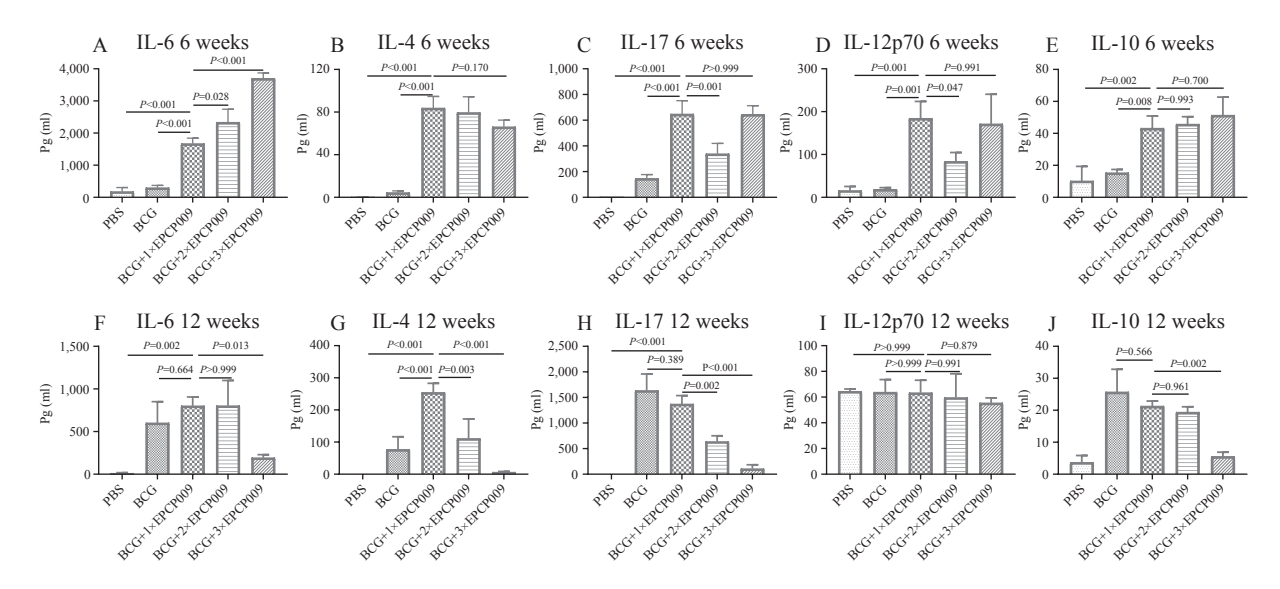
^{*} Corresponding author: Haican Liu, liuhaican@icdc.cn.

National Key Laboratory of Intelligent Tracking and Forecasting for Infectious Diseases, National Institute for Communicable Disease

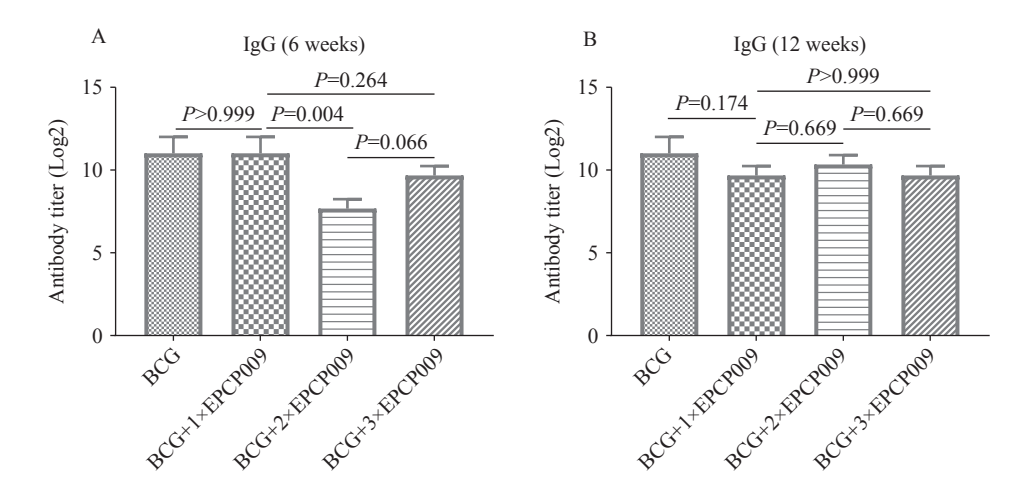
China CDC Weekly

- candidates. Vaccine 2023;41(26):3836 46. https://doi.org/10.1016/j.vaccine.2023.04.003.
- 13. Hatherill M, White RG, Hawn TR. Clinical development of new TB vaccines: recent advances and next steps. Front Microbiol 2019;10: 3154. https://doi.org/10.3389/fmicb.2019.03154.
- Shurygina AP, Zabolotnykh N, Vinogradova T, Khairullin B, Kassenov M, Nurpeisova A, et al. Preclinical evaluation of TB/FLU-04l-an intranasal influenza vector-based boost vaccine against tuberculosis. Int J Mol Sci 2023;24(8):7439. https://doi.org/10.3390/ijms24087439.
- Fan XT, Li XY, Wan KL, Zhao XQ, Deng YL, Chen ZX, et al. Construction and immunogenicity of a T cell epitope-based subunit vaccine candidate against *Mycobacterium tuberculosis*. Vaccine 2021;39 (47):6860 – 5. https://doi.org/10.1016/j.vaccine.2021.10.034.
- Moguche AO, Musvosvi M, Penn-Nicholson A, Plumlee CR, Mearns H, Geldenhuys H, et al. Antigen availability shapes T cell differentiation and function during tuberculosis. Cell Host Microbe 2017;21(6):695 706.e5. https://doi.org/10.1016/j.chom.2017.05. 012.

SUPPLEMENTARY MATERIAL



SUPPLEMENTARY FIGURE S1. Levels of cytokines secreted by PPD-stimulated spleen lymphocytes in mice 6 and 12 weeks from initial immunization. (A) IL-6, (B) IL-4, (C) IL-17, (D) IL-12 and (E) IL-10 secreted at 6 weeks; (F) IL-6, (G) IL-4, (H) IL-17, (I) IL-12 and (J) IL-10 secreted at 12 weeks.



SUPPLEMENTARY FIGURE S2. Antibody responses in BALB/c mice immunized with BCG, BCG+1×EPCP009, BCG+2×EPCP009, and BCG+3×EPCP009 at (A) 6 weeks and (B) 12 weeks.

Methods and Applications

Evaluation of Measles Vaccine Immunogenicity and Durability Using A Pseudotyped Virus Neutralization Assay

Qi Jiang¹; Xi Wu¹; Jie Zhang¹; Huiling Wang²; Fangyu Dong³; Xuelian Wu¹; Pengju Yu¹; Jianhui Nie¹; Youchun Wang⁴; Weijin Huang¹; Jiuyue Zhou³; Yaru Quan⁵; Yan Zhang².#; Suting Wang⁶.#; Juan Li⁵.#

ABSTRACT

Introduction: This study aimed to establish a robust method for monitoring measles vaccine-induced immunity and assessing population-level serostatus.

Methods: This study constructed a vesicular stomatitis virus (VSV)-based pseudotyped virus system expressing envelope proteins from seven major circulating measles genotypes (H1, B3, D4, D8, D9, D11, G3) and the Schwarz vaccine strain (genotype A), thereby enabling a high-throughput neutralization assay for antibody detection.

Results: Vaccination induced a substantial increase in neutralizing antibody geometric mean titers (GMT) post-immunization (4,808 after the first dose; 5,326 after the second dose), with antibody levels remaining elevated in 4-year-old children (GMT: 3,834). Crossneutralization activity against different genotypes varied by less than 6.4-fold, demonstrating broad protective immunity. However, 12% of adult sera tested were seronegative, revealing the presence of susceptible populations.

Conclusions: This study confirms the robust immunogenicity of the current measles vaccine and establishes a valuable tool for serosurveillance and long-term immunity assessment.

Measles virus (MeV) is a highly contagious pathogen that spreads rapidly through airborne transmission, with a basic reproduction number (R0) ranging from 12 to 18. Consequently, localized outbreaks or large-scale epidemics can emerge when the proportion of susceptible individuals exceeds 10%. Prior to the introduction of measles vaccination, the virus caused millions of deaths worldwide each year (1).

The Edmonston wild-type strain, isolated in 1954, serves as the ancestral virus for the measles vaccine used globally. The first-generation measles attenuated

vaccine (Edmonston strain B) derived from this strain received approval in the United States in 1963. Despite the availability of a safe and effective measles vaccine for decades and global immunization programs achieving approximately 86% coverage among target populations, measles remains a leading cause of childhood mortality worldwide, particularly among children under five years of age (2). Using measles case data reported by countries to the World Health Organization (WHO) and the United Nations Children's Fund (UNICEF), the research team led by Anna A. Minta and Matt Ferrari developed an estimation model for measles cases and deaths. According to their model, the estimated annual number of measles deaths declined from 800,000 in 2000 to 107,500 in 2023, representing an 87% reduction. However, in recent years, factors including the coronavirus disease 2019 (COVID-19) pandemic, economic instability, natural disasters, famine, and population displacement have caused stagnation or declines in routine and supplementary immunization coverage, resulting in a continuous increase in measles cases (3). According to the latest data from the WHO and the U.S. CDC, an estimated 10.3 million measles cases occurred globally in 2023, representing a 20% increase compared to 2022, with approximately 108,000 associated deaths. Outbreaks were reported in all WHO regions except the Americas, with nearly half of the cases occurring in Africa. From March 1, 2024, to February 28, 2025, a total of 28,791 measles cases were reported in the European Union, with 86% occurring in unvaccinated individuals. Between January 1 and March 20, 2025, the United States reported 378 measles cases, with at least 75% occurring in unvaccinated individuals (4).

Measles eradication depends on achieving and maintaining high vaccination coverage to sustain herd immunity. Consequently, continuous surveillance of population-level measles antibody titers, coupled with timely supplementary and booster vaccination of unvaccinated or susceptible individuals, is critically

important. However, conventional enzyme-linked immunosorbent assays (ELISA) suffer from limited specificity and susceptibility to environmental interference, whereas plaque reduction neutralization tests (PRNT) are constrained by low throughput and extended testing durations (5). To overcome these limitations, we developed a reliable, stable, rapid, and highly specific pseudotyped virus-based in vitro neutralization assay for detecting measles-neutralizing This method complements existing antibodies. serological assays and was applied to evaluate population immunity levels and assess both the immunogenicity and durability of the current measles vaccine.

METHODS

Plasmids, Sera, and Cells

The hemagglutinin (H) protein (GenBank: AAA56657.1) and fusion (F) protein (GenBank: AAA56656.1) genes from the measles virus (MeV) vaccine strain Schwarz, together with the H and F gene sequences from seven circulating strains — B3 (KT732216.1), D4 (JN635402.1), D8 (KT732231.1), (KY969476.1), D11 (MN017369.1), (KC164758.1), and H1 (ON035899.1) — as well as one sequenced virus isolate, were codon-optimized and individually cloned into the pcDNA3.1 vector. This cloning strategy generated the pcDNA3.1-H and pcDNA3.1-F expression constructs, respectively (Supplementary Figure S1, available at https://weekly. chinacdc.cn/).

A total of 42 serum samples were collected from infants and young children at four time points: before measles-mumps-rubella (MMR) vaccination, after the first dose, after the second dose, and at 4 years of age. These samples were obtained through the Shandong CDC. Additionally, 50 adult serum samples were collected from Shandong Taibang Biological Products Co., Ltd. All samples were collected under protocols ensuring donor safety and maintaining complete anonymization of personal identifying information.

Mouse sera were collected at week 6 following an immunization regimen that consisted of an initial dose of MeV H protein DNA vaccine, followed by two booster immunizations with measles pseudotyped virus administered at two-week intervals.

Twenty-one cell lines were cultured for this study: HEK 293T, MRC5, A549, HeLa, SK-N-MC, Hep2, HepG2, Huh7, Vero, LLC-MK2, CHO, BHK21,

NIH3T3, MDCK, Cf2TH, Mv1Lu, PK15, MDBK, CRFK, and Vero-SLAM. All cells were maintained in Dulbecco's Modified Eagle Medium (DMEM) or the manufacturer-recommended medium supplemented with 100 U/mL penicillin-streptomycin (GIBCO) and 10% fetal bovine serum (FBS; Pansera ES, PAN-Biotech) at 37 °C in a humidified atmosphere containing 5% CO₂.

HEK 293T cells were stably transfected with NECTIN4 and SLAM receptor genes to generate stable cell lines designated 293T-NECTIN4 and 293T-SLAM, respectively. These cell lines were established through antibiotic selection using 1.5 mg/L puromycin and 150 mg/L hygromycin B, respectively.

Pseudotyped Virus Packaging

HEK 293T cells were transfected with a mixture of pcDNA3.1-H and pcDNA3.1-F plasmids at a 4:1 ratio using the Lipofectamine 3000 Transfection Kit (Invitrogen, USA) following the manufacturer's protocol. Six hours post-transfection, cells were infected with 6-9G* Δ G-GFP VSV pseudotyped virus for 4 hours. Culture supernatants containing pseudotyped virus were harvested 24 hours post-infection and clarified by centrifugation at 4,000 ×g for 10 minutes at 4 °C. The clarified supernatants were then filtered through 0.45 µm sterile membranes, aliquoted, and stored at –80 °C until use.

Pseudotyped Virus Titration

Serial 3-fold dilutions of MeV-GFP pseudotyped virus stock (50 μ L per well) were prepared in 96-well clear cell-culture plates. Each well received 100 μ L of 293T-NECTIN4 cell suspension (4×10⁵ cells/mL), and plates were incubated for 24 hours at 37 °C in a humidified atmosphere containing 5% CO₂. GFP-positive cells were enumerated using a fluorescence cell counter (Cytation 5, BioTek), and viral titers were expressed as focus-forming units per milliliter (FFU/mL).

Pseudotyped Virus Neutralization

Samples were initially diluted 1:30 in 96-well plates, followed by 3-fold serial dilutions. MeV-GFP pseudotyped virus was added at a multiplicity of infection (MOI) of 1.4, and the mixture was incubated at 37 °C with 5% CO $_2$ for 1 hour. Subsequently, 100 μL of 293T-NECTIN4 cell suspension (4×10 5 cells/mL) was added to each well, and plates were incubated for 24 hours at 37 °C with 5% CO $_2$. GFP-

positive cells were quantified using a BioTek fluorescence reader. The 50% neutralization titer (NT $_{50}$) was calculated using the Reed-Muench method to determine neutralizing antibody levels in the samples (6).

Microneutralization Experiments

The 25 μ L serum sample was subjected to 2-fold serial dilution in 96-well microplates and were mixed with 25 μ L of 100 TCID $_{50}$ measles virus. The mixture was incubated at 37 °C with 5% CO $_2$ for 90 minutes. Subsequently, 100 μ L of Vero-SLAM cell suspension at a density of 1–1.5 × 10 5 cells/mL was added to each well. Plates were incubated at 37 °C with 5% CO $_2$ for 2 to 5 days (typically 3 days) to monitor cytopathic effects (CPE). The antibody titer was defined as the highest serum dilution that completely inhibited CPE.

RESULTS

Selection of Viral Strains

We retrieved representative circulating measles virus genotypes (B3, D4, D8, D9, D11, G3, H1) from the MeaNS database based on recent epidemiological surveillance data. These strains, together with the vaccine strain (genotype A), underwent nucleotide sequence analysis of the hemagglutinin (H) gene to construct a phylogenetic tree and assess genetic

distances. Following screening for strains with complete H and F protein sequences, we generated pseudotyped viruses representing eight distinct genotypes. Amino acid sequence analysis of the H protein revealed that the phylogenetic tree clustered into nine distinct groups (Supplementary Figure S2A, available at https://weekly.chinacdc.cn/). The eight representative strains selected exhibited H protein sequences of 618 amino acid residues with 93.53% to 98.22% identity (Supplementary Figure S2).

NECTIN4 and SLAM Receptors Enhance Measles Virus Infectivity

To evaluate receptor-dependent infectivity, we challenged 21 cell lines derived from eight host species with the MeV pseudotyped virus (genotype H1). These included 10 human, 2 monkey, 3 mouse, and 2 canine cell lines, as well as one each from mink, pig, cattle, and cat origins. Among these, two cell lines stably overexpressing receptors — 293T-NECTIN4 and 293T-SLAM — were included for comparison. As shown in Figure 1, the MeV pseudotyped virus failed to infect parental 293T cells but efficiently infected 293T-NECTIN4 and 293T-SLAM cells. Infection of other cell lines was either minimal or absent, demonstrating that NECTIN4 and SLAM receptors are essential for MeV pseudotyped virus entry. Since 293T-NECTIN4 cells exhibited the highest infection rate, this cell line was selected for all

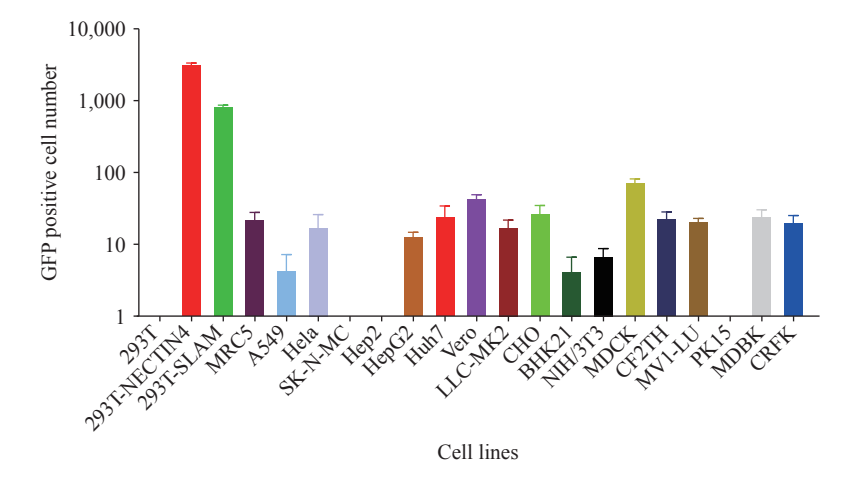


FIGURE 1. Infectivity of measles pseudotyped virus in different cell lines. Abbreviation: 293T=human embryonic kidney cells; 293T-NECTIN4=human embryonic kidney cells expressing NECTIN4; 293T- SLAM=human embryonic kidney cells expressing SLAM; MRC5=human lung fibroblast cells; A549=human lung cancer cells; HeLa=human cervical cancer cells; SK-N-MC=human neuroblastoma cell line; Hep2=human larynx epidermal carcinoma cell line; HepG2=human hepatocellular carcinoma cells; Huh-7=human hepatocellular carcinoma cells; Vero=African green monkey kidney cells; LLC-MK2=Rhesus monkey kidney cells; CHO=Chinese hamster ovary cells; BHK21=baby hamster kidney cells; NIH-3T3=mouse embryo fibroblast cells; MDCK=canine kidney cells; CF2TH=canine thymus cells; MV1-LU=mink cell line; PK15=pig kidney cell line; MDBK=bovine kidney cells.

subsequent pseudotyped virus experiments (Figure 1).

The x-axis indicates the different cell lines tested, and the y-axis represents the log₁₀ number of GFP-positive cells produced following incubation with the measles virus pseudotyped virus.

Establishment and Validation of the Pseudotyped Virus Neutralization Assay

To establish a robust in vitro neutralization assay using measles pseudotyped virus, we systematically optimized key assay parameters, including cell seeding density $(1.6 \times 10^2 \text{ to } 3.2 \times 10^5 \text{ cells/well})$, pseudotyped virus input (MOI ranging from 0.017 to 114), and incubation duration (8 to 120 hours). Our results demonstrated that the number of GFP-positive cells increased proportionally with higher cell seeding densities. NT₅₀ remained stable across the cell density range of 1.6×10² to 4×10⁴ cells/well, with linear correlation coefficients (R²) consistently exceeding 0.995 within the 1.3×10^3 to 4×10^4 cells/well range. Based on these findings, we selected 4×10⁴ cells/well as the optimal cell density for subsequent assays (Figure 2A and 2B). When the pseudotyped virus MOI ranged from 0.017 to 1.4, NT₅₀ values remained stable, achieving an R² of 0.998 at MOI=1.4. Consequently, an MOI of 1.4 was chosen for all further experiments (Figure 2C). GFP-positive cell counts increased with extended incubation time and reached a plateau after 60 hours. NT₅₀ values remained stable between 12 and 120 hours, with R² values exceeding 0.999 during the 24- to 60-hour window. To optimize the balance between assay accuracy and time efficiency, we selected a 24-hour post-infection incubation period as the optimal detection time (Figure 2D and 2E).

To validate the assay's reliability, we systematically evaluated multiple performance parameters: cut-off value, specificity, linearity, dynamic range, robustness, precision, and correlation with the authentic virus neutralization test. The cut-off value was established at 150, derived from the mean plus three standard deviations (mean + 3SD=154) of negative serum samples (Figure 2F). Measles antibody-positive sera exclusively exhibited neutralizing activity against the measles pseudotyped virus, confirming high assay specificity (Figure 2G). Within an inhibition range of 20% to 90%, the assay demonstrated a robust linear relationship between sample dilution and response (R²>0.92) (Figures 2H and 2I). We further validated the method's robustness by systematically varying

experimental conditions: incubation time of the pseudovirus from 0.5 h to 1.5 h (Figure 2J), different batches of pseudovirus (Figure 2K), 1 to 3 freeze-thaw cycles of the pseudovirus (Figure 2L), and 1 to 3 freeze-thaw cycles of the serum samples (Figure 2M). For each condition, three serum samples were subjected to three independent experiments, with six replicates per experiment. Minor variations in experimental parameters resulted in NT₅₀ values within a twofold range, confirming excellent assay robustness. Repeated measurements of identical samples yielded intra-assay coefficients of variation (CV) ranging from 6.1% to 19.8% and inter-assay CVs between 10.6% and 17.1%, demonstrating strong assay precision (Figure 2N). Finally, correlation analysis of 42 serum samples tested by both the pseudotyped virus assay and the authentic virus microneutralization test revealed a strong positive correlation (y=0.756x+1.852, r=0.85), confirming excellent agreement between the two methods.

Cross-protection by Antibodies Against Different Genotypes of Measles Virus

To assess the potential for immune escape among different measles virus strains, we selected genotypes H1 and B3 for animal immunization and performed neutralization assays using pseudotyped viruses representing eight measles virus genotypes with the corresponding immunized mouse sera. Sera from H1immunized mice exhibited average neutralizing antibody titers (NT₅₀) against genotypes A, H1, B3, D4, D8, D9, D11, and G3 of 2,863; 18,316; 7,286; 12,570; 8,602; 6,011; 4,004; and 12,378, respectively. from B3-immunized mice demonstrated corresponding NT₅₀ values of 4,437; 12,227; 17,525; 16,234; 14,155; 11,923; 5,693; and 16,182, respectively. Notably, the variation in neutralization titers across different genotypes did not exceed 6.4fold. Given that all antibody titers remained substantially above the protection threshold, current vaccines provide full protection against diverse circulating strains (Figure 3).

Vaccine Evaluation

To assess the immunogenicity, durability, and cross-protective efficacy of the measles vaccine against various genotypes, we performed neutralization assays using sera collected from 42 individuals at four time points: pre-vaccination (8 months of age), after the first dose of MMR vaccine, after the second dose, and

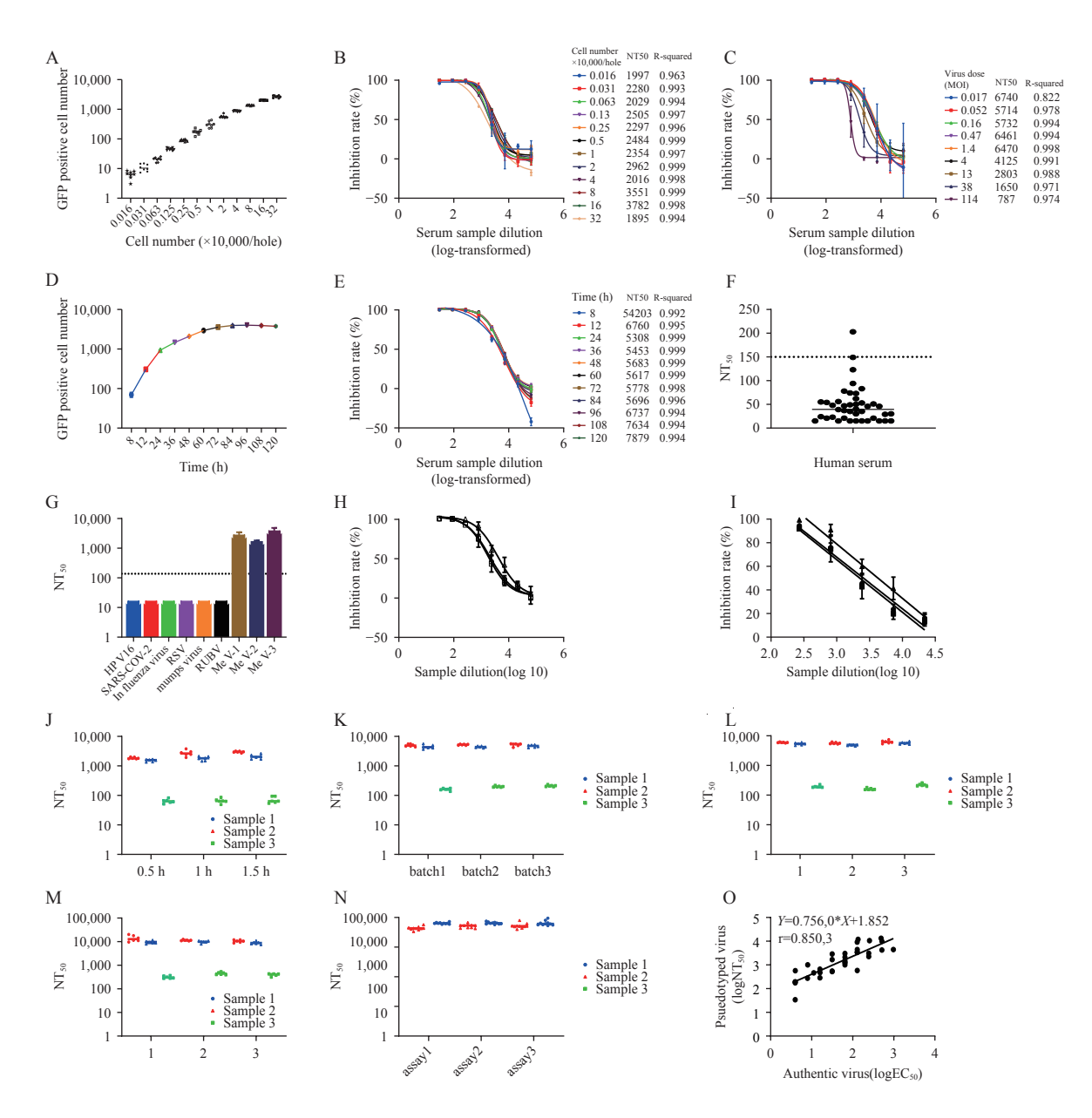


FIGURE 2. Establishment and validation of an in vitro neutralizing antibody detection method based on measles pseudotyped virus. (A) Effect of varying cell seeding densities on measles pseudotyped virus titration; (B) Effect of different cell seeding densities on measles pseudotyped virus neutralization; (C) Effect of varying pseudotyped virus input amounts on neutralization; (D) Effect of different incubation times on measles pseudotyped virus titration; (E) Effect of different incubation times on neutralizing antibody detection using the measles pseudotyped virus assay; (F) Determination of the cut-off value for the in vitro neutralizing antibody assay; (G) Specificity validation of the neutralization assay; (H) Linear range assessment of the neutralizing antibody assay; (I) Linearity assessment of the neutralizing antibody assay. Robustness of the assay under varying experimental conditions: (J) incubation time of the pseudovirus varied from 0.5 to 1.5 hours; (K) different batches of pseudovirus were used; (L) pseudovirus underwent 1 to 3 freeze—thaw cycles; (M) serum samples underwent 1 to 3 freeze—thaw cycles; (N) Precision assessment of the neutralizing antibody assay; (O) Correlation between the pseudotyped virus neutralization assay developed in this study and the gold-standard live virus neutralization assay.

Note: For (M), 3 serum samples were subjected to three independent experiments, with 6 replicates per experiment.

at 4 years of age. The geometric mean neutralizing antibody titers (NT_{50}) were 48, 4,808, 5,326, and 3,834, respectively. Compared to pre-vaccination sera, antibody levels increased approximately 100-fold after

the first dose, 110-fold after the second dose, and remained 80-fold higher at 4 years, demonstrating robust immunogenicity and sustained immunity. Student's *t*-test was performed to examine sex-based

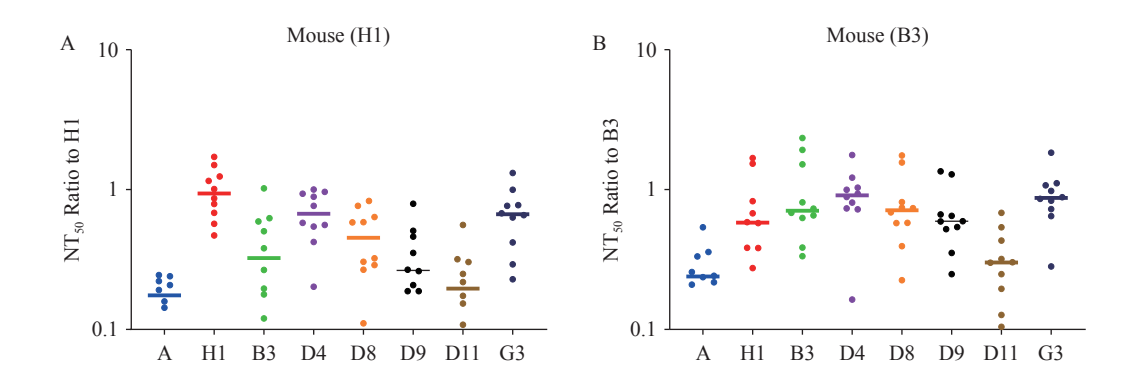


FIGURE 3. Cross-neutralization of measles pseudotyped virus. (A) Neutralization assay of measles pseudotyped viruses representing different genotypes using sera from mice immunized with the H1 genotype. (B) Neutralization assay of measles pseudotyped viruses representing different genotypes using sera from mice immunized with the B3 genotype. Note: For (A), the x-axis indicates the various measles pseudotyped virus genotypes, and the y-axis shows the fold change in NT₅₀ values relative to H1 genotype-elicited serum. For (B), the x-axis indicates the various measles pseudotyped virus genotypes, and the y-axis shows the fold change in NT₅₀ values relative to B3 genotype-elicited serum.

differences at each time point. No significant differences in antibody levels were observed between male and female subjects across all groups (Figure 4A–E).

MMR-vaccinated sera demonstrated average neutralizing titers against genotypes A, H1, B3, D4, D8, D9, D11, and G3 of 3,929; 6,330; 4,046; 7,482; 5,373; 3,575; 2,241; and 8,390, respectively. The lowest neutralization titer was observed against genotype D11, with only a 1.8-fold difference compared to other genotypes, indicating that the current vaccine confers protective immunity against diverse circulating measles virus strains (Figure 4F).

Antibody Levels in Adults

To assess measles virus antibody levels in the general population, we performed the pseudotyped virus neutralization assay on 50 adult serum samples. The geometric mean neutralizing antibody titer among adults was 1,322, with 12% (6/50) of sera falling below the detection threshold, highlighting the need to strengthen herd immunity. When samples were stratified by age and sex, Duncan's Multiple Range Test revealed no significant differences in measles antibody levels among the adult cohorts (Figure 5).

DISCUSSION

Measles is recognized as one of the most important targets for global eradication due to the high efficacy and widespread availability of the measles vaccine, combined with the virus having a single serotype and no animal reservoir (7). The core strategy for measles control and elimination involves establishing and

maintaining herd immunity through high vaccine coverage, thereby interrupting viral transmission and reducing measles-related mortality. In recent years, global health organizations have achieved significant progress in expanding measles vaccination coverage and controlling outbreaks through sustained efforts. However, in certain countries and regions, factors including vaccine hesitancy, insufficient healthcare infrastructure, and socioeconomic challenges have contributed to declining vaccination rates. Suboptimal vaccine coverage has resulted in measles resurgence and outbreaks, including the reestablishment of endemic transmission in countries where measles had previously been eliminated (8). Between 2022 and 2023, the estimated number of global measles cases increased by 20%. In 2023, 57 countries experienced large-scale or disruptive measles outbreaks, defined by the IA2030 global monitoring framework as ≥20 cases per million inhabitants, representing a 58% increase in affected countries compared to 2022. Among these countries, 47% (27 outbreaks) occurred in the African region, 23% (13 outbreaks) in the Eastern Mediterranean region, 18% (10 outbreaks) in the European region, 7% (4 outbreaks) in the Western Pacific region, and 5% (3 outbreaks) in the Americas (9). With progress in global measles elimination efforts, the diversity of circulating strains has declined substantially. Genotypes D11, B2, G3, D9, H1, and D4 were last detected in 2010, 2011, 2014, 2019, 2019, and 2020, respectively (10). Currently, only genotypes B3 and D8 remain endemic, exhibiting distinct regional distributions: B3 predominates in Africa, the Americas, and the Eastern Mediterranean, whereas D8 represents the main genotype in Europe, Southeast Asia, and the

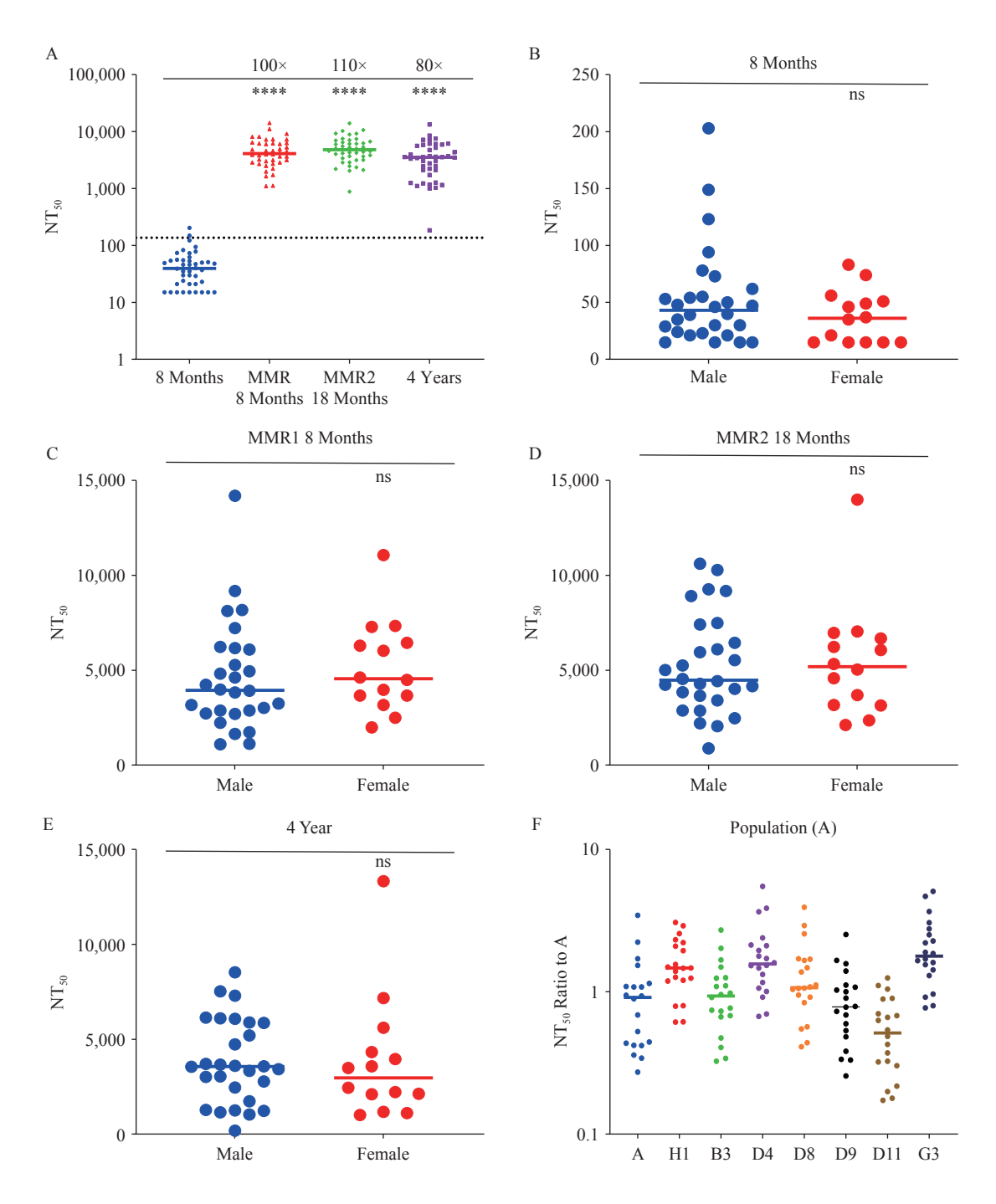


FIGURE 4. Determination of vaccine-induced measles antibody levels. (A) Overall measles neutralizing antibody levels in infant sera across vaccination time points. (B) Pre-vaccination measles antibody levels stratified by sex. (C) Post-first-dose measles antibody levels stratified by sex. (D) Post-second-dose measles antibody levels stratified by sex. (E) Measles antibody levels in 4-year-old children stratified by sex. (F) Cross-neutralization of measles pseudotyped viruses representing diverse genotypes by vaccinated sera.

Note: ns means no significant difference. For (A), the x-axis represents four groups based on serum collection timing: pre-MMR vaccination (8 months), post-first dose (8 months), post-second dose (18 months), and at 4 years of age. The y-axis displays NT_{50} values. Duncan's Multiple Range Test was applied for group comparisons. For (B), The x-axis distinguishes male and female groups, while the y-axis represents NT_{50} values; Student's *t*-test was performed. For (C, D, and E), the x-axis distinguishes male and female groups, while the y-axis represents NT_{50} values; Student's *t*-test was performed. For (F), The x-axis indicates measles pseudotyped virus genotypes, and the y-axis displays relative NT_{50} values normalized to the vaccine strain (genotype A).

Abbreviation: NT_{50} =50% neutralizing antibody titer. **** P<0.001.

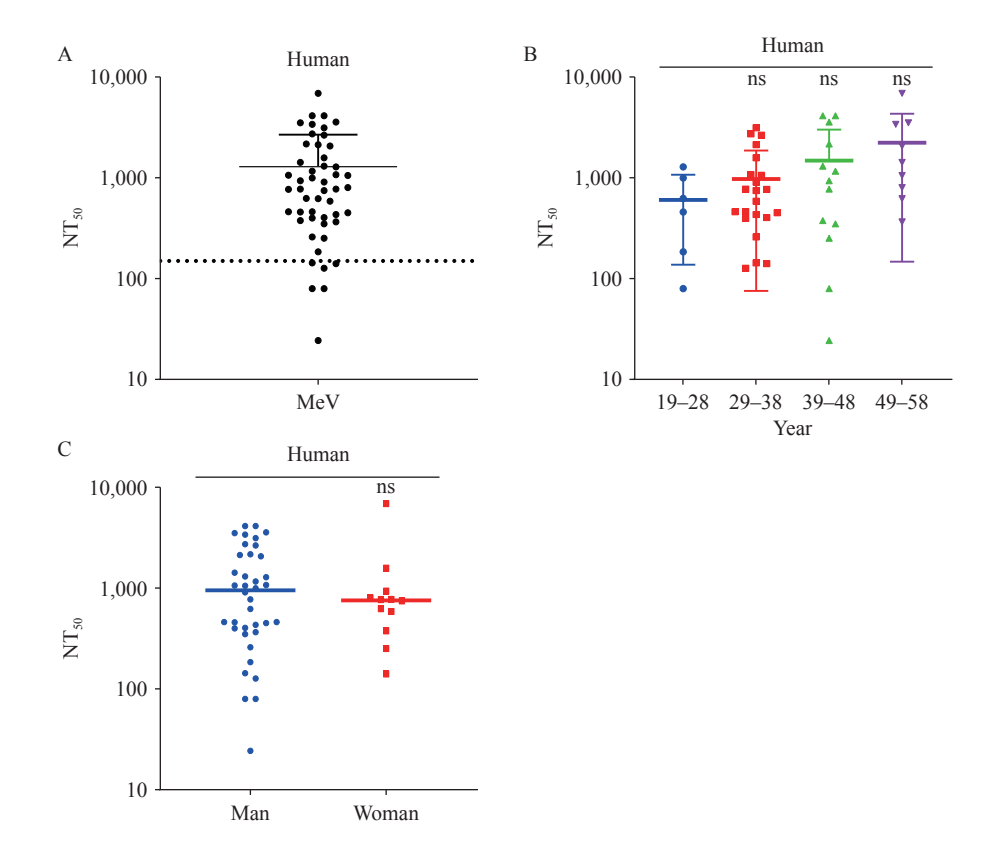


FIGURE 5. Detection of serum measles antibody levels in adults. (A) Overall measles neutralizing antibody levels in adult sera. The y-axis indicates NT50 values. (B) Measles antibody levels in adult sera stratified by age. (C) Measles antibody levels in adult sera stratified by sex.

Note: ns means no significant difference. For (A), the 50 adult samples were divided into five age groups spanning 10 years each (19–28, 29–38, 39–48, and 49–58 years). The y-axis indicates NT50 values; Duncan's Multiple Range Test was performed among groups. For (C), the y-axis indicates NT50 values; Student's t-test was performed. Abbreviation: NT50=50% neutralizing antibody titer.

Western Pacific (Supplementary Figure S3, available at https://weekly.chinacdc.cn/).

Our study demonstrated that immune sera elicited by measles virus genotypes H1 and B3 exhibited robust cross-NT₅₀ against the other seven genotypes, with not exceeding 6.4-fold and differences consistently maintained above 150. These findings demonstrate significant cross-neutralization among different genotypes and indicate that current vaccines provide effective protection against all circulating strains. The regional distribution of genotypes is therefore not attributed to immune escape but is primarily associated with low vaccination coverage and the susceptibility of individuals or populations lacking neutralizing antibodies. Previous research has suggested that the epitope recognized by MAb-BH26 represents the most important immunodominant epitope, as MAb-BH26 inhibits the binding of approximately 60% of human serum antibodies in both convalescent measles patients and vaccinees (11). The binding site of MAb-BH26 is predicted to reside within either the

amino acid region 571-579 or 190-200, with both potentially contributing recognition. Notably, the residues at positions 191–195 are located in close proximity to the receptorbinding site (RBS) and interact directly with SLAM (12). These residues are 100% conserved across all eight strains tested in our study. Furthermore, amino acids 379-400 have been identified as forming an immunodominant epitope known hemagglutinating and noose epitope (HNE) (13). The cysteines at positions 386 and 394 are critical for maintaining its conformational integrity. Among the strains examined in our study, cysteines at positions 386 and 394 are completely conserved, with only variations occurring in other residues. Therefore, the high sequence conservation at these immunodominant sites likely explains the absence of immune escape among circulating measles virus genotypes.

We established the cut-off value for neutralization assays using pre-vaccination sera from 8-month-old

infants as negative controls (14). Compared to prevaccination baseline levels, measles antibody titers increased approximately 100-fold and 110-fold after the first and second doses of the MMR vaccine, respectively, demonstrating strong immunogenicity. At 4 years of age, antibody levels remained elevated, approximately 80-fold higher than pre-vaccination levels, indicating durable immunity. Additionally, neutralization assays performed with 50 adult plasma samples revealed residual antibody levels 28-fold higher than those observed in pre-vaccination infant sera. However, only 88% (44/50) of adult sera exhibited antibody titers above the detection threshold, highlighting the risk of susceptible individuals accumulating in the population and underscoring the critical need to strengthen herd immunity. These findings are consistent with research conducted by Minghao Zhou's team (15).

These findings demonstrate that regions and countries where measles has not been fully eliminated must accelerate efforts to increase vaccine coverage and ensure broader population immunity for achieving herd protection. Furthermore, enhanced surveillance and reporting systems are essential for the prompt detection and control of outbreaks. In countries and regions where measles has been successfully eliminated, continued vigilance through active monitoring and rapid response measures remains critical to prevent disease resurgence.

In summary, this study establishes a rapid, safe, convenient, automatable, and standardized *in vitro* neutralization assay utilizing pseudotyped measles virus. This assay can be effectively applied to monitor antibody levels in susceptible populations and evaluate vaccine immunogenicity. The method holds significant promise for large-scale, population-wide antibody surveillance, which will facilitate the assessment of measles epidemiology, outbreak risk prediction, and acceleration of global measles elimination efforts.

Ethical statement: Pathogen testing for infants and young children approval by the Medical Ethics Committee of the Shandong Provincial Center for Disease Control and Prevention [SDJK(K)2024-053-01]. Mouse experiments were conducted under approval from the Institutional Animal Care and Use Committee at the National Institutes for Food and Drug Control (NIFDC) [2024(B)048]. Human serum samples were collected with informed consent for pathogen marker detection.

Conflicts of interest: No conflicts of interest.

Funding: Supported by the Major Project of

Guangzhou National Laboratory, Grant No. GZNL2024A01019.

doi: 10.46234/ccdcw2025.224

* Corresponding authors: Juan Li, lijuan@nifdc.org.cn; Suting Wang, sdsjbyfkzzx-mys@shandong.cn; Yan Zhang, zhangyan@ivdc.chinacdc.cn.

Copyright © 2025 by Chinese Center for Disease Control and Prevention. All content is distributed under a Creative Commons Attribution Non Commercial License 4.0 (CC BY-NC).

Submitted: July 22, 2025 Accepted: September 25, 2025 Issued: October 17, 2025

REFERENCES

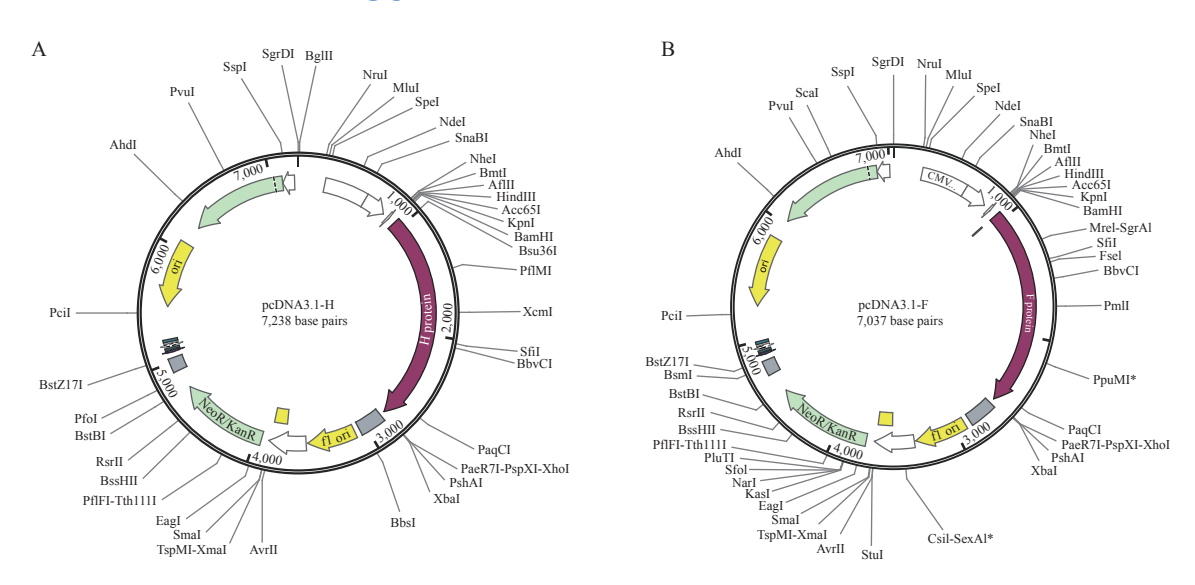
- Moss WJ. Measles. Lancet 2017;390(10111):2490 502. https://doi. org/10.1016/S0140-6736(17)31463-0.
- Ikegame S, Hashiguchi T, Hung CT, Dobrindt K, Brennand KJ, Takeda M, et al. Fitness selection of hyperfusogenic measles virus F proteins associated with neuropathogenic phenotypes. Proc Natl Acad Sci USA 2021;118(18):e2026027118. https://doi.org/10.1073/pnas. 2026027118.
- Bidari S, Yang W. Global resurgence of measles in the vaccination era and influencing factors. Int J Infect Dis 2024;147:107189. https://doi. org/10.1016/j.ijid.2024.107189.
- 4. WHO. Measles United States of America. 2025. https://www.who.int/emergencies/disease-outbreak-news/item/2025-DON561. [2025-3-27]
- Lutz CS, Hasan AZ, Bolotin S, Crowcroft NS, Cutts FT, Joh E, et al. Comparison of measles IgG enzyme immunoassays (EIA) versus plaque reduction neutralization test (PRNT) for measuring measles serostatus: a systematic review of head-to-head analyses of measles IgG EIA and PRNT. BMC Infect Dis 2023;23(1):367. https://doi.org/10.1186/ s12879-023-08199-8.
- Liang ZT, Wu X, Wu JJ, Liu S, Tong JC, Li T, et al. Development of an automated, high-throughput SARS-CoV-2 neutralization assay based on a pseudotyped virus using a vesicular stomatitis virus (VSV) vector. Emerg Microbes Infect 2023;12(2):e2261566. https://doi.org/10.1080/ 22221751.2023.2261566.
- Rota PA, Moss WJ, Takeda M, de Swart RL, Thompson KM, Goodson JL. Measles. Nat Rev Dis Primers 2016;2(1):16049. https://doi.org/10. 1038/nrdp.2016.49.
- Tahir IM, Kumar V, Faisal H, Gill A, Kumari V, Tahir HM, et al. Contagion comeback: unravelling the measles outbreak across the USA. Front Public Health 2024;12:1491927. https://doi.org/10.3389/fpubl. 2024 1491927
- 9. Minta AA, Ferrari M, Antoni S, Lambert B, Sayi TS, Hsu CH, et al.

¹ Division of HIV/AIDS and Sexually Transmitted Virus Vaccines, Institute for Biological Product Control, State Key Laboratory of Drug Regulatory Science, National Institutes for Food and Drug Control (NIFDC), Beijing, China; ² WHO Western Pacific Regional Measles/Rubella Reference Laboratory, National Key Laboratory for Intelligent Tracking and Forecasting of Infectious Diseases, NHC Key Laboratory of Medical Virology and Viral Diseases, National Institute for Viral Disease Control and Prevention, Chinese Center for Disease Control and Prevention, Beijing, China; ³ Department of Research & Development, Taibang Biologics Group, Beijing, China; ⁴ Institute of Medical Biology, Chinese Academy of Medical Sciences, Kunming City, Yunnan Province, China; ⁵ Division of Respiratory Virus Vaccines, National Institutes for Food and Drug Control, Beijing, China; ⁶ Shandong Center for Disease Control and Prevention, Jinan City, Shandong Province, China.

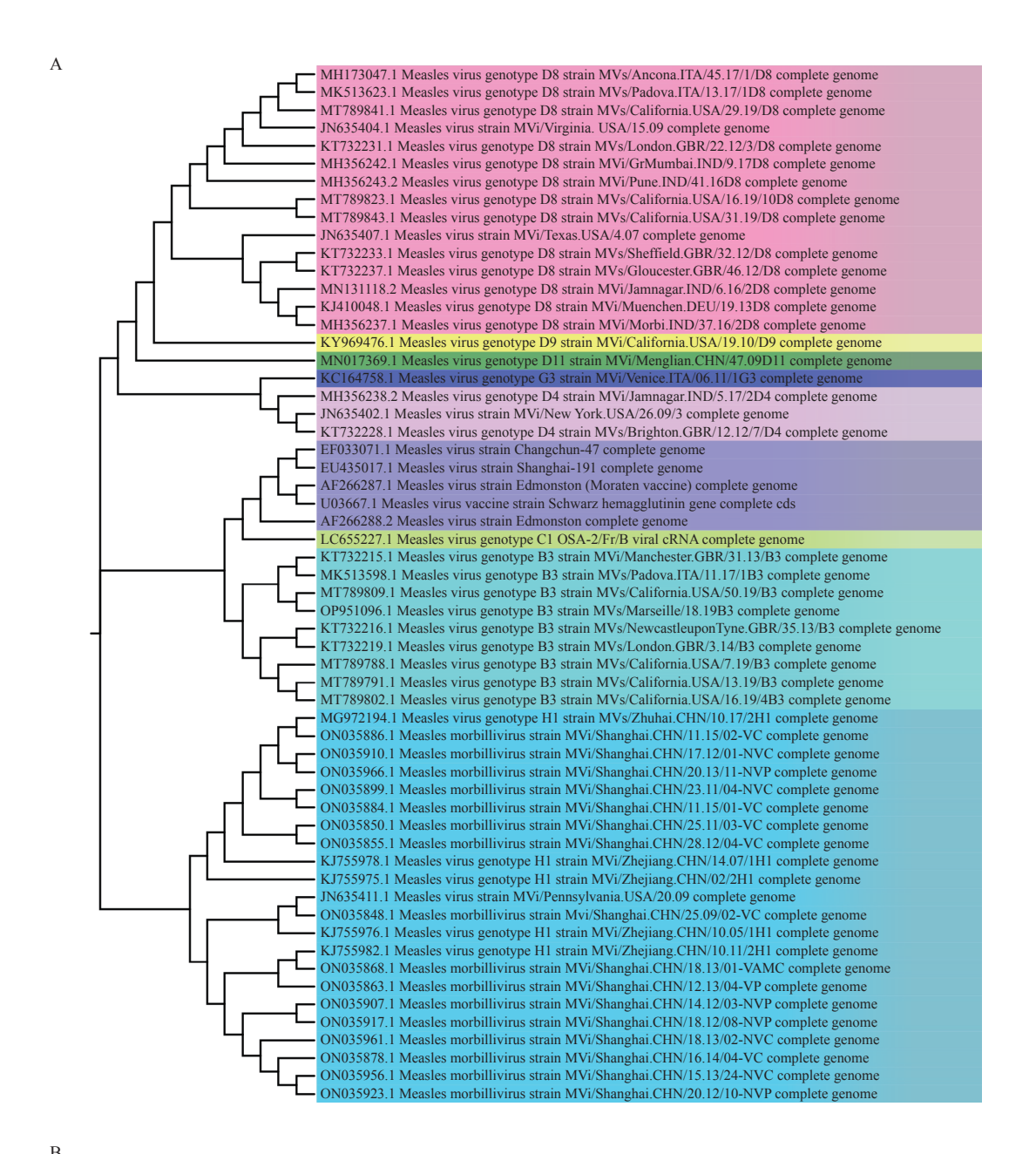
China CDC Weekly

- Progress toward measles elimination worldwide, 2000–2023. MMWR Morb Mortal Wkly Rep 2024;73(45):1036 42. https://doi.org/10.15585/mmwr.mm7345a4.
- Bankamp B, Kim G, Hart D, Beck A, Ben Mamou M, Penedos A, et al. Global update on measles molecular epidemiology. Vaccines 2024;12 (7):810. https://doi.org/10.3390/vaccines12070810.
- 11. Ertl OT, Wenz DC, Bouche FB, Berbers GAM, Muller CP. Immunodominant domains of the Measles virus hemagglutinin protein eliciting a neutralizing human B cell response. Arch Virol 2003;148(11):2195 206. https://doi.org/10.1007/s00705-003-0159-9.
- Hashiguchi T, Ose T, Kubota M, Maita N, Kamishikiryo J, Maenaka K, et al. Structure of the measles virus hemagglutinin bound to its cellular receptor SLAM. Nat Struct Mol Biol 2011;18(2):135 41. https://doi.org/10.1038/nsmb.1969.
- Ziegler D, Fournier P, Berbers GAH, Steuer H, Wiesmüller KH, Fleckenstein B, et al. Protection against measles virus encephalitis by monoclonal antibodies binding to a cystine loop domain of the H protein mimicked by peptides which are not recognized by maternal antibodies. J Gen Virol 1996;77(10):2479 – 89. https://doi.org/10. 1099/0022-1317-77-10-2479.
- 14. Wang QL, Wang W, Winter AK, Zhan ZF, Ajelli M, Trentini F, et al. Long-term measles antibody profiles following different vaccine schedules in China, a longitudinal study. Nat Commun 2023;14(1): 1746. https://doi.org/10.1038/s41467-023-37407-x.
- Hu Y, Lu PS, Deng XY, Guo HX, Zhou MH. The declining antibody level of measles virus in China population, 2009-2015. BMC Public Health 2018;18(1):906. https://doi.org/10.1186/s12889-018-5759-0.

SUPPLEMENTARY MATERIAL



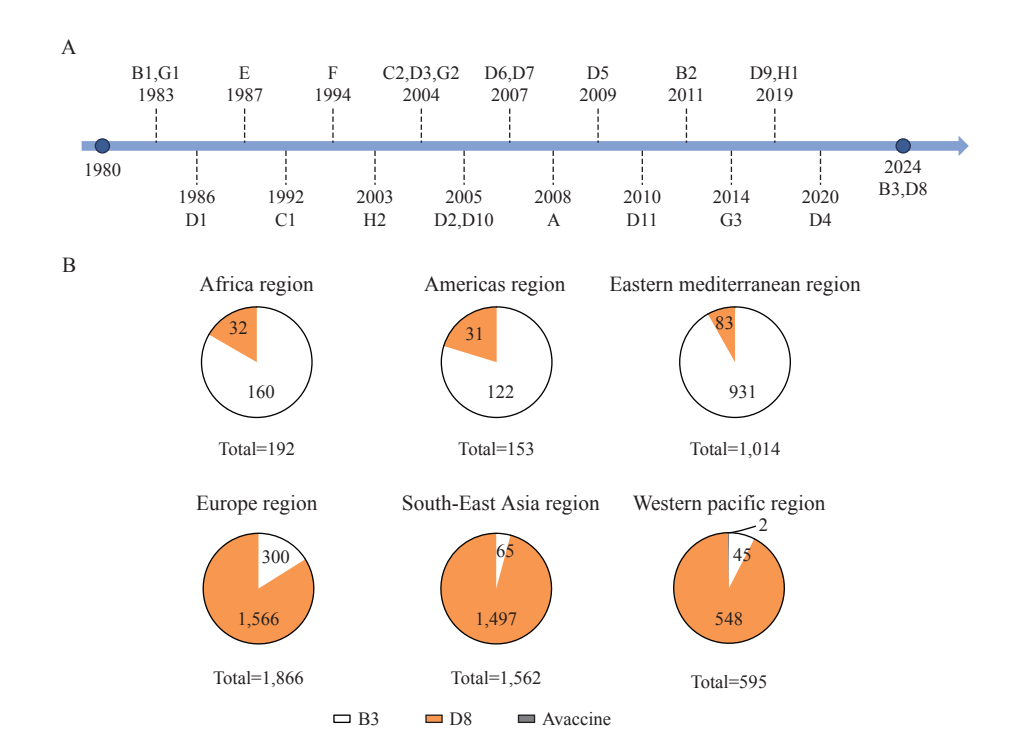
SUPPLEMENTARY FIGURE S1. Vector maps of expression plasmids. (A) Vector map of plasmid pcDNA3.1-H. (B) Vector map of plasmid pcDNA3.1-F.



NSPORDR | NAFYKONPHEKGSR | V | NREHLM | DRPYYLLAYLFVMFLSL | GLLA | AG | RLHRAA! YTAE | HKSLSTNLDVTNS | EHQVKDVLTPLFK | | GDEVGLRTPQRFTDLVKE | SDK | KFLNPDREYDFRDLTWC | NPPER | KLDYDQYCADVAAEELMNALVNSTLLEABATVQFLAVSKGNCSGPTT | RGQFSN | NSLSLLDLYLSBGYNVSS | YTMTSQGNYGGTYLVEKPNLSKGSELSQLSMARVFEVGY | RNPGLGAPVFHWTNYFEQPYSADESNCWVALGELKEAALC | HSEDS | T | PYQGSGKGVSFQLVKLGVWKSPTDMQSWVPLSTDDPY | DRLYLSSHBGV | ADNQAKWAYPTTRTDDKLRMETCFQQACKGK | QALCENEEWAPLKDAR | PSYGYLSVBLSLTYELK | K | ASGFGPL | THGSGNDLYKSNENNAYWLT | PPMKNLALGV | NTLEW | PREKVSP-LFTVP | KEAGEDCHAPTYLPAEVDGDVKLSSNLV | LPGQDLQYVLATYDTSRVEHAVVYYVYSPSRSFSYFYPFRLP | KGYP | ELQVECFTVDQKLWCRHFCVLADSESGGH | THSGNV GNGVSCTXTREDGTNRR

SUPPLEMENTARY FIGURE S2. Measles virus H protein sequence analysis. (A) Phylogenetic tree constructed using nucleotide sequences of the H protein from 58 measles virus strains. (B) Amino acid sequence analysis of the H protein from eight selected measles virus strains.

China CDC Weekly



SUPPLEMENTARY FIGURE S3. Global distribution and temporal trends of measles virus genotypes. (A) Most recent detection year for each of the 24 measles virus genotypes documented in the MeaNS database. (B) Geographic circulation patterns of measles virus genotypes between January 2022 and December 2023. Note: Data source are MeaNS2 database (Genotypes).

Youth Editorial Board

Director Lei Zhou

Vice Directors Jue Liu Tiantian Li Tianmu Chen

Members of Youth Editorial Board

Jingwen Ai Li Bai Yuhai Bi Yunlong Cao Gong Cheng Liangliang Cui Meng Gao Jie Gong Yuehua Hu Xiang Huo Jia Huang Xiaolin Jiang Yu Ju Min Kang Huihui Kong Lingcai Kong Shengjie Lai Fangfang Li Jingxin Li **Huigang Liang** Di Liu Jun Liu Li Liu Yang Liu Chao Ma Yang Pan Zhixing Peng Menbao Qian Tian Qin Shuhui Song Kun Su Song Tang Bin Wang Jingyuan Wang Linghang Wang Qihui Wang Feixue Wei Xiaoli Wang Xin Wang Yongyue Wei Zhiqiang Wu Meng Xiao Tian Xiao Wuxiang Xie Lei Xu Lin Yang Canging Yu Lin Zeng Yi Zhang Yang Zhao Hong Zhou

Indexed by Science Citation Index Expanded (SCIE), Social Sciences Citation Index (SSCI), PubMed Central (PMC), Scopus, Chinese Scientific and Technical Papers and Citations, and Chinese Science Citation Database (CSCD)

Copyright © 2025 by Chinese Center for Disease Control and Prevention

Under the terms of the Creative Commons Attribution-Non Commercial License 4.0 (CC BY-NC), it is permissible to download, share, remix, transform, and build upon the work provided it is properly cited. The work cannot be used commercially without permission from the journal. References to non-China-CDC sites on the Internet are provided as a service to CCDC Weekly readers and do not constitute or imply endorsement of these organizations or their programs by China CDC or National Health Commission of the People's Republic of China. China CDC is not responsible for the content of non-China-CDC sites.

The inauguration of *China CDC Weekly* is in part supported by Project for Enhancing International Impact of China STM Journals Category D (PIIJ2-D-04-(2018)) of China Association for Science and Technology (CAST).



Vol. 7 No. 42 Oct. 17, 2025

Responsible Authority

National Disease Control and Prevention Administration

Sponsor

Chinese Center for Disease Control and Prevention

Editing and Publishing

China CDC Weekly Editorial Office No.155 Changbai Road, Changping District, Beijing, China Tel: 86-10-63150501, 63150701 Email: weekly@chinacdc.cn

CSSN

ISSN 2096-7071 (Print) ISSN 2096-3101 (Online) CN 10-1629/R1